Colloquium: Bulk Bogoliubov excitations in a Bose-Einstein condensate

R. Ozeri,* N. Katz, J. Steinhauer,† and N. Davidson

Department of Physics of Complex Systems, Weizmann Institute of Science, Rehovot 76100, Israel

(Published 8 April 2005)

Bogoliubov theory for excitations in Bose-Einstein condensates was formulated over 50 years ago to qualitatively explain strongly interacting superfluids. Quantitative experimental verification of this theory came with the long-awaited realization of gaseous, weakly interacting condensates. This Colloquium reviews recent experimental advances in the study of Bogoliubov bulk excitations in Bose-Einstein condensates, obtained using two-photon Bragg scattering.

CONTENTS

I. INTRODUCTION

Unlike many other phase transitions, interactions are not required for Bose-Einstein condensation (BEC) to occur. Einstein's 1925 paper predicted the occurrence of BEC in a completely ideal gas of bosons (Einstein, 1925). Little theoretical effort was invested in BEC during the years following Einstein's prediction, since BEC was regarded as not much more than a theoretical anecdote. Progress was eventually motivated, however, by the study of superfluid ^{4}He.

Fritz London's 1938 hypothesis, relating the normal to superfluid transition to Bose-Einstein condensation (London, 1938), motivated the theoretical study of interacting Bose degenerate fluids and the comparison between the theoretical predictions and the results of the experimental study of liquid ^{4}He. London was able to give a fairly accurate prediction for the λ temperature based on the theoretical value of the critical temperature for Bose-Einstein condensation, the mass of ^{4}He atoms, and the liquid density. Shortly after, Tisza used the notion of BEC in his two fluid model (Tisza, 1938). This model, describing the co-existence of a thermal and a condensate phase in the fluid, qualitatively explained the superfluid fountain effect and predicted the existence of second sound (temperature waves).

In his 1941 paper, Landau formulated a phenomenological description of superfluids as a weakly interacting mixture of excitations such as phonons and rotons (Landau, 1941). Landau rejected London's and Tisza's point of view, based on the argument that in such highly interacting systems the use of an ideal gas description is inadequate. Years passed before the measurement of the excitation spectrum of superfluid ^{4}He. This spectrum is indeed in complete disagreement with the free particle, parabolic spectrum assumed by Tisza's two-fluid model. Despite the fact that it was not derived from microscopic arguments, Landau's excitation spectrum turned out to be correct.

The Bogoliubov theory for excitations in a weakly interacting Bose gas presented a breakthrough in the understanding of Landau's excitation spectrum, despite the fact that a weakly interacting gas is a crude approximation to liquid ^{4}He. Roughly 60 years ago, in his seminal work, Bogoliubov used field theoretical methods to present a basis in which the Hamiltonian of a weakly interacting gas of bosons is diagonal (Bogoliubov, 1947). The Bogoliubov basis describes excitations that exhibit a

*Present address: Time and Frequency Division, NIST, Boulder, Colorado 80305, USA. Electronic address: ozeri@boulder.nist.gov

†Present address: Department of Physics, Technion–Israel Institute of Technology, Technion City, Haifa 32000, Israel.

phononlike, linear dispersion at low momentum. In this sense, Bogoliubov theory reconciles the two different points of view (London-Tisza vs Landau), as it shows that the quantum-mechanical description of a weakly interacting Bose gas features both Bose-Einstein condensation and a phonon excitation spectrum.

In 1958, Beliaev showed that the system's Hamiltonian, when taken to a higher order than Bogoliubov theory, describes interactions between the different Bogoliubov excitations (Beliaev, 1958). These interactions give rise to the finite lifetime of Bogoliubov excitations.

Despite the fact that they describe a weakly interacting gas, the theories of Bogoliubov and Beliaev provide qualitative explanations for features of the strongly interacting superfluid ^{4}He, including superfluidity itself. The discrepancy in the quantitative results, however, is unavoidable. The experimental verification of these theories came with the long awaited realization of the gaseous, weakly interacting BEC (Anderson *et al.*, 1995; Davis *et al.*, 1995).

Low-lying Bogoliubov excitations were experimentally and theoretically studied almost immediately after the realization of BEC. As Bogoliubov and Beliaev theories were formulated for a homogeneous condensate, further theoretical work was needed to incorporate inhomogeneous trapped condensates into Bogoliubov theory (Edwards *et al.*, 1996; Pérez-García *et al.*, 1996; Stringari, 1996). By perturbing the trapping potential at the proper excitation frequency, the condensate is excited into one of the low-lying Bogoliubov modes (Jin *et al.*, 1996; Mewes *et al.*, 1996; Fort *et al.*, 2000; Onofrio *et al.*, 2000). The lifetime of these excitations is limited by Beliaev and Landau damping processes (Jin *et al.*, 1997; Pitaevskii and Stringari, 1997; Giorgini, 1998; Stamper-Kurn *et al.*, 1998). Beautiful experiments have also shown engineered Beliaev coupling between excitations in two discrete, low-lying modes (Hodby *et al.*, 2001).

In 1999, Ketterle's group at MIT used the technique of two-photon Bragg transitions to excite and spectroscopically probe excitations in BEC (Stamper-Kurn *et al.*, 1999; Stenger *et al.*, 1999). Two-photon Bragg transitions impart a well-defined momentum $\hbar k$ to the condensate. As condensates are usually harmonically trapped, k is not a good quantum number, and therefore it is a superposition of Bogoliubov modes that is being excited. This introduces a faster decay rate of the Bragg-driven excitation due to dephasing between these different Bogoliubov modes. However, because of the relatively high momentum imparted in such transitions, the excitation wavelength can be made much shorter than the condensate size. In this case high-energy modes are excited, and the spread in energies of excited modes relative to their average energy becomes small. Moreover, control over the frequency difference between the Bragg beams enables selectivity in the energies that are excited. Typically, Bragg-driven excitations are not in the low-lying discrete regime mentioned above, but are part of a quasicontinuum of modes. Owing to their short wavelength, the nature of these excitations is dominated by the "bulk" properties of the condensate rather than the condensate geometry. The comparison of these experiments with Bogoliubov theory, which was initially formulated for a homogenous infinite condensate, is quite good. Thus the disadvantage of Bragg-driven excitations, namely k not being a good quantum number, is compensated by their expository value, a linear dependence of the phonon energy on k being but one example.

In contrast to Beliaev coupling in the low-lying discrete case, Beliaev damping in the Bragg regime couples modes into a quasicontinuum of modes. This, as we plan to show in the following, forms an analogy between a macroscopically populated Bogoliubov mode, which is coupled to a quasicontinuum of modes through its interaction with the ground-state condensate, and a laser beam which is coupled to the electromagnetic vacuum through the presence of an atom. As in the atom-laser system, bosonic amplification can play an important role by emphasizing a certain mode over the continuum.

The experimental study of Bogoliubov excitations in BEC is paramount for the understanding of these quantum degenerate gases. The spectrum of excitations carries information on microscopic properties of the condensate, such as second-order density correlation, which confirms the condensate is of gaseous nature, as well as macroscopic properties such as the speed of sound and the critical velocity for superfluidity in the condensate.

In this Colloquium we review the experimental progress made during the last few years in the study of weak excitations in BEC by means of photon scattering, in the limit of zero temperature. These experiments were performed with both sodium (Stamper-Kurn *et al.*, 1999; Stenger *et al.*, 1999; Vogels *et al.*, 2002) and rubidium (Katz *et al.*, 2002; Ozeri *et al.*, 2002; Steinhauer *et al.*, 2002, 2003) Bose-Einstein condensates.

II. CONDENSATE GROUND STATE

Bose-Einstein condensation is a statistical phase transition, at the end of which practically all of the atoms in a weakly interacting gas of bosons occupy the quantum ground state of the gas. Therefore a Bose-Einstein condensate can be fully described by the wave function $\psi(\mathbf{r}_1,\mathbf{r}_2,\ldots,\mathbf{r}_{N_0})$, which is the ground-state solution to the many-body Schrodinger equation,

$$H\psi(\mathbf{r}_1,\mathbf{r}_2,\ldots,\mathbf{r}_{N_0}) = E\psi(\mathbf{r}_1,\mathbf{r}_2,\ldots,\mathbf{r}_{N_0}). \tag{1}$$

A variational calculation can be used to minimize the energy expectation value $\int \psi^\dagger H\psi d^{N_0}\mathbf{r}$ with respect to ψ, under the condition that the number of atoms in the gas is constant, i.e., $\int \psi^\dagger\psi d^{N_0}\mathbf{r} = N_0$. Assuming a contact atomic interaction potential and that the many-body wave function ψ can be factorized into a product of identical states ϕ for all atoms, the variational minimization leads to ϕ being the solution of the well-known Gross-Pitaevskii (GP) equation (Castin, 2001),

$$\left(-\frac{\hbar^2}{2m}\nabla^2 + V_{\text{ext}}(\mathbf{r}) + g|\phi(\mathbf{r})|^2\right)\phi(\mathbf{r}) = \mu\phi(\mathbf{r}), \tag{2}$$

where $g = 4\pi\hbar^2 a/m$, a is the s-wave scattering length, m

is the atomic mass, and $n(\mathbf{r})=|\phi(\mathbf{r})|^2$ is the condensate density at the point $\mathbf{r}$. The three terms in the parentheses on the left-hand side of Eq. (2) account for three different contributions to the condensate energy. The first term accounts for the kinetic energy of the gas, and is related to the inverse size of the condensate through the Heisenberg uncertainty relation. The second term is the confining potential. For an infinite, homogeneous condensate these first two terms vanish. The third term represents the energy resulting from atom-atom interactions. For positive g this latter energy is larger in higher density regions. This atom-atom interaction term introduces nonlinearity into the equation of state for the gas. Owing to the nonlinearity of the Gross-Pitaevski equation μ is not equal to E/N_0, the energy per particle in the gas, but rather represents the condensate's chemical potential $\mu=dE/dN_0$ (Castin, 2001).

For an infinite homogenous condensate $\mu=gn$. This interaction energy leads to the introduction of a new length scale,

$$\xi=\hbar/\sqrt{2mgn}. \tag{3}$$

The healing length ξ is the minimal distance over which the condensate wave function can vary significantly.

For a sufficiently large number of atoms, the kinetic energy term can be neglected in Eq. (2) in what is known as the Thomas-Fermi (TF) approximation (Dalfovo *et al.*, 1999). In the Thomas-Fermi regime Eq. (2) is reduced to an algebraic form that gives the condensate density $n(\mathbf{r})=(1/g)[V_{\text{ext}}(\mathbf{r})-\mu]$ for regions where $V_{\text{ext}}<\mu$, and $n(\mathbf{r})=0$ outside this region. When $V_{\text{ext}}(\mathbf{r})$ is a harmonic trapping potential, the condensate profile is that of an inverted parabola. The linear size of the condensate radial, or axial, dimensions, is referred to as R_{TF}, the Thomas-Fermi radius.

III. BOGOLIUBOV EXCITATIONS

Since the Gross-Pitaevski equation is a nonlinear equation of state, the energy of an excitation will depend on the excitation population. The notion an excitation spectrum can be retained only in the limit of excitations that are perturbations over the ground state. In such a case the interaction between different excitations is small compared to the interaction between an excitation and the undepleted ground state. One can therefore linearize the Gross-Pitaevski equation with respect to the excitation wave function, leading to the Bogoliubov theory (Bogoliubov, 1947).

Even though realizable trapped condensates are inhomogeneous, for expository value the first subsection will describe excitations in an infinite and homogeneous condensate. The second subsection will deal with Bogoliubov theory for the more general case of excitations in a trapped, inhomogeneous condensate.

A. Bogoliubov theory—Homogeneous condensates

It is useful to describe Bogoliubov theory using second quantization. Taking only two-body interactions into account, we write the second-quantized Hamiltonian for a cold gas of N interacting atoms,

$$\hat{H}=\sum_{\mathbf{k}}\epsilon_k^0\hat{a}_{\mathbf{k}}^\dagger\hat{a}_{\mathbf{k}}+\frac{g}{2V}\sum_{\mathbf{k1},\mathbf{k2},\mathbf{k3},\mathbf{k4}}\hat{a}_{\mathbf{k1}}^\dagger\hat{a}_{\mathbf{k2}}^\dagger\hat{a}_{\mathbf{k3}}\hat{a}_{\mathbf{k4}}\delta_{\mathbf{k1}+\mathbf{k2},\mathbf{k3}+\mathbf{k4}}. \tag{4}$$

$\hat{a}_{\mathbf{k}}^\dagger$ and $\hat{a}_{\mathbf{k}}$ are the creation and annihilation operators, respectively, of atoms with momentum $\hbar\mathbf{k}$, $\epsilon_k^0=(\hbar\mathbf{k})^2/2m$ is the free-particle kinetic energy, and V is the volume of the gas. Since our atoms are bosons, $\hat{a}_{\mathbf{k}}^\dagger$ and $\hat{a}_{\mathbf{k}}$ obey the bosonic commutation relations,

$$[\hat{a}_{\mathbf{k}},\hat{a}_{\mathbf{k}'}^\dagger]=\delta_{\mathbf{k},\mathbf{k}'},[\hat{a}_{\mathbf{k}},\hat{a}_{\mathbf{k}'}]=[\hat{a}_{\mathbf{k}}^+,\hat{a}_{\mathbf{k}'}^\dagger]=0. \tag{5}$$

The first term in Eq. (4) counts the number of atoms having momentum $\hbar\mathbf{k}$, and allocates to each one of them the corresponding kinetic energy, ϵ_k^0. The second term in Eq. (4) describes collisions between pairs of atoms. The δ function ensures momentum conservation. As expected, the coupling constant for an S-wave collision is independent of the relative momentum.

We now wish to neglect the depletion of the $k=0$ mode, and replace $\hat{a}_0^\dagger$ and $\hat{a}_0$ by their classical expectation value $\sqrt{N_0}$. For this approximation to be valid, two conditions must be fulfilled. First, interactions should be weak enough that the depletion of the $k=0$ mode in the ground state is small, meaning that the number of atoms in an "interaction volume" is small, i.e., $na^3\ll 1$. Based on the Bogoliubov approximation, it can be shown that the quantum depletion of the ground state of a homogeneous condensate is proportional to $\sqrt{na^3}$ (Fetter, 1998), demonstrating the self-consistency of the approximation. The second condition of Bogoliubov theory is the assumption of few excitations, allowing us to neglect (for now) all the terms below N_0 order.

Under these assumptions, the Hamiltonian of the gas can be diagonalized with a canonical transformation to the Bogoliubov quasiparticle basis,

$$\hat{a}_{\mathbf{k}}=u_k\hat{b}_{\mathbf{k}}-v_k\hat{b}_{-\mathbf{k}}^\dagger$$

$$\hat{a}_{-\mathbf{k}}^\dagger=u_k\hat{b}_{-\mathbf{k}}^\dagger-v_k\hat{b}_{\mathbf{k}}, \tag{6}$$

given that u_k and v_k satisfy

$$u_k^2=v_k^2+1=\frac{1}{2}\left(\frac{\epsilon_k^0+gn}{\epsilon_k}+1\right), \tag{7}$$

where ϵ_k is the Bogoliubov quasiparticle energy, given by

$$\epsilon_k=\sqrt{\epsilon_k^0(\epsilon_k^0+2gn)}=gn\sqrt{(k\xi)^2[(k\xi)^2+2]}. \tag{8}$$

u_k and v_k, the Bogoliubov quasiparticle amplitudes, are real, positive, and isotropic.

The atomic composition of the Bogoliubov vacuum is resolved by looking at the expectation value of different

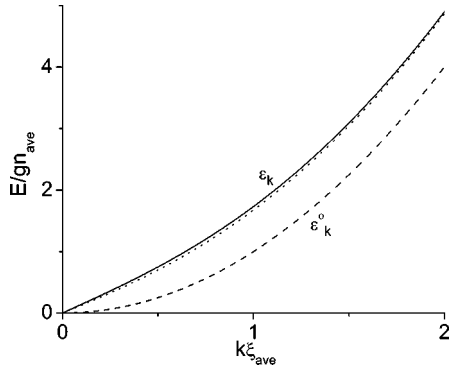

FIG. 1. The Bogoliubov quasiparticle energy, plotted as a function of $k\xi$: solid line, for a homogeneous condensate; dotted line, the local-density approximation (cf. Sec. V.C below); dashed line, the free-particle kinetic energy. The energy is normalized by the average density of the condensate, and the healing length is evaluated at the average density.

atomic number operators, with respect to the vacuum state, yielding $\langle \hat{a}_k^\dagger \hat{a}_k \rangle = \langle \hat{a}_{-k}^\dagger \hat{a}_{-k} \rangle = v_k^2$. This isotropic distribution of v_k^2 atoms moving with momentum k, is the quantum depletion of the condensate ground state.

According to Eq. (6), an excitation is composed only of atoms moving either with momentum $\hbar\mathbf{k}$ or $-\hbar\mathbf{k}$. The atomic composition of an excitation is found by taking the expectation value of the atomic number operators, and subtracting v_k^2. We find $\langle \hat{a}_k^\dagger \hat{a}_k \rangle - v_k^2 = u_k^2$, and $\langle \hat{a}_{-k}^\dagger \hat{a}_{-k} \rangle - v_k^2 = v_k^2$. Thus Bogoliubov quasiparticles can be thought of as composed of u_k^2 atoms moving in the excitation direction, and v_k^2 atoms moving opposite to the excitation direction. Although the total number of atoms that compose a single excitation can be large, according to Eq. (7), the net momentum carried by a single excitation is equal to $\hbar k$.

The solid line in Fig. 1 shows the Bogoliubov energy for a homogeneous condensate Eq. (8) as a function of $k\xi$. The dashed line indicates the free particle parabolic dispersion. Two regimes are evident in the spectrum. For $k\xi < 1$ the Bogoliubov dispersion is roughly linear,

$$\epsilon_k \approx ck, \tag{9}$$

where $c = \sqrt{gn/m}$ is the condensate speed of sound. This linear regime of the spectrum is referred to as the phonon regime. In the phonon regime $v_k^2, u_k^2 \approx 1/2k\xi > 1$. Phonons are therefore collective excitations which can involve a large number of particles. Excitations in the phonon regime correspond to sound waves that propagate in the condensate with velocity c.

In an MIT experiment (Vogels *et al.*, 2002), the Bogoliubov amplitudes u_k^2 and v_k^2 were observed for phonons, with $k\xi = 0.38$, as shown in Fig. 2. This corresponds to the amplitudes $u_k^2 = 1.53$ and $v_k^2 = 0.53$. Since the density of the condensate was inhomogenous, these values are calculated in the local density approximation (LDA), discussed in Sec. V.C. In Fig. 2, the height of the left (right) peak is proportional to v_k^2 (u_k^2). This measurement was

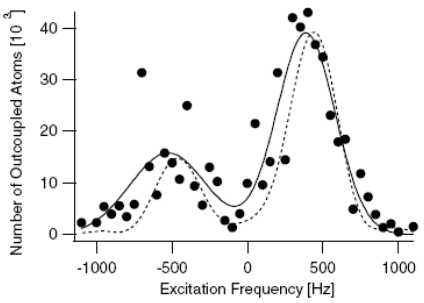

FIG. 2. The measured Bogoliubov amplitudes. The measurement, indicated by circles, was performed for phonons with $k\xi = 0.38$. The height of the left peak is proportional to v_k^2 and that of the right peak to u_k^2. The solid curve is a sum of two Gaussians. The dashed curve is the LDA result. From Vogels *et al.*, 2002.

performed using Bragg spectroscopic techniques, as suggested in Brunello *et al.* (2000). Bragg spectroscopy will be discussed in Sec. V.

For $k\xi > 1$ the Bogoliubov dispersion is roughly quadratic, and is shifted by a constant value from the free-particle parabola,

$$\epsilon_k \approx \epsilon_k^0 + gn. \tag{10}$$

In this single-particle regime $u^2 \approx 1$ and $v^2 \approx 0$. Consequently the Bogoliubov excitations are single-particle excitations. gn is the extra energy required for these atoms to move with momentum $k\xi > 1$. Atoms moving at high momenta have twice the interaction energy of atoms in the $k = 0$ state.

The linear dependence of ϵ_k on $\mu = gn$ given by Eq. (10) was verified experimentally, as indicated by the

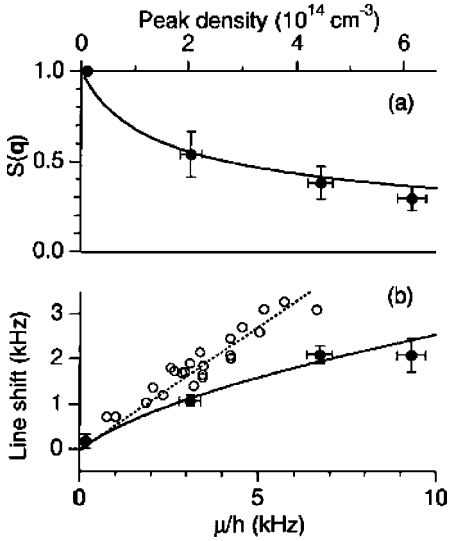

FIG. 3. The density dependence of (a) the static structure factor, and (b) the quasiparticle energy, for a k value corresponding to $\epsilon_k^0 = h \times 1.38$ kHz. The filled circles are the measured values. The solid curves are the LDA results. The dotted curve and open circles are the single-particle values for $\epsilon_k^0 = h \times 100$ kHz, as in Fig. 6(a). From Stamper-Kurn *et al.*, 1999.

open circles of Fig. 3(b), which show $\epsilon_k - \epsilon_k^0$ for $\epsilon_k^0 = h \times 100$ kHz. Since this value of ϵ_k^0 is much larger than the values of μ shown in the figure, the open circles are within the single-particle regime. The open circles were taken from the MIT group's experiment (Stenger *et al.*, 1999), and are also shown in Fig. 6(a).

B. Bogoliubov theory—Inhomogeneous condensates

Bogoliubov theory was generalized in the early 1960s, by Gross (1961) and Pitaevskii (1961), to the case of inhomogeneous, trapped gases. The time evolution of the condensate wave-function in the mean-field approximation is given by

$$i\hbar\frac{\partial}{\partial t}\Phi(\mathbf{r},t) = \left(-\frac{\hbar^2}{2m}\nabla^2 + V_{\text{ext}}(\mathbf{r}) + g|\Phi(\mathbf{r},t)|^2\right)\Phi(\mathbf{r},t), \tag{11}$$

which is known as the time-dependent Gross-Pitaevskii equation. The time-independent Gross-Pitaevski equation, Eq. (2), can be extracted from Eq. (11) by making the ansatz $\Phi(\mathbf{r},t) = e^{-i(\mu/\hbar)t}\phi(\mathbf{r})$.

Bogoliubov excitations can be studied by inserting into Eq. (11) a solution that has small corrections to the ground-state wave function (Pitaevskii, 1961; Dalfovo *et al.*, 1999),

$$\Phi(\mathbf{r},t) = e^{-i(\mu/\hbar)t}[\phi(\mathbf{r}) + u(\mathbf{r})e^{-i\omega t} + v^*(\mathbf{r})e^{i\omega t}], \tag{12}$$

where $u(\mathbf{r})$ and $v(\mathbf{r})$ are the Bogoliubov quasiparticle amplitudes. Substituting Eq. (12) into Eq. (11), and keeping terms linear in $u(\mathbf{r})$ and $v(\mathbf{r})$, we obtain the Bogoliubov coupled equations,

$$\hbar\omega u(\mathbf{r}) = [H_0 - \mu + 2g\phi^2(\mathbf{r})]u(\mathbf{r}) + g\phi^2(\mathbf{r})v(\mathbf{r}),$$

$$-\hbar\omega v(\mathbf{r}) = [H_0 - \mu + 2g\phi^2(\mathbf{r})]v(\mathbf{r}) + g\phi^2(\mathbf{r})u(\mathbf{r}), \tag{13}$$

where $H_0 = -(\hbar^2/2m)\nabla^2 + V_{\text{ext}}(\mathbf{r})$. The spectrum of solutions of Eq. (13) gives the excitation spectrum of the condensate.

Analytic solutions to the Bogoliubov equations are attainable only for very special cases, such as a homogeneous condensate (no trapping potential), or a spherically symmetric harmonic potential in the Thomas-Fermi limit, where kinetic energy can be neglected even for the excitation wave function (Stringari, 1996). Generally, the Bogoliubov coupled equations have to be integrated numerically (Edwards *et al.*, 1996; Pérez-García *et al.*, 1996). Both analytic solutions in the Thomas-Fermi limit and numerical solutions have been compared with experiments performed on low-lying excitations, and have been found to be in excellent agreement (Jin *et al.*, 1996; Mewes *et al.*, 1996; Matthews *et al.*, 1998; Fort *et al.*, 2000; Onofrio *et al.*, 2000).

One special case for which the solutions to Eq. (13) are of particular interest is that of an infinitely long cylinder that is harmonically bound in the radial direction, since realizable condensates in the laboratory, even though harmonically bound in all dimensions, are often cylindrically symmetric and very elongated. The excitation spectrum of an infinite cylinder thus carries many of the qualitative features of the spectrum of elongated condensates (Steinhauer *et al.*, 2003).

The zero azimuthal angular momentum solutions to Eq. (13) for an infinite cylinder are of the form (Hutchinson and Zaremba, 1998; Stringari, 1998; Tozzo and Dalfovo, 2003)

$$(u,v)_{n,k}(\rho,z) = \frac{1}{\sqrt{L}}e^{ikz}(u,v)_{n,k}(\rho). \tag{14}$$

L is the length of the condensate in the axial direction z, and is taken to infinity, while keeping N/L, the number of atoms per unit length, constant. The excitation wave function is seen to be factored into two terms, plane waves in the axial direction, which are characterized by the continuous quantum number k, and radial functions $(u,v)_{n,k}(\rho)$. The radial quantum number n enumerates the number of nodes in u and v in the radial direction. The amplitudes $(u,v)_{n,k}(\rho)$ are found by a numerical integration of Eq. (13) with Eq. (14). For the case of an infinite cylinder, linear momentum is a good quantum number in the axial direction. However, momentum can be imparted in the axial direction in different radial modes, each having a different energy. This is analogous to the propagation of electromagnetic radiation in a waveguide.

IV. INTERACTIONS BETWEEN EXCITATIONS

In Bogoliubov theory, the many-body Hamiltonian is truncated to terms that are proportional to N_0, whereas terms describing the coupling between different excitations are at most proportional to $\sqrt{N_0}$ and are therefore $\sqrt{N_0}$-fold suppressed. Nevertheless, the effect of excitation-excitation coupling can hardly be ignored. For excitations with large quantum numbers, e.g., high k, the number of excitation modes to which an excitation in mode k can couple can be very large. When this number is comparable to $\sqrt{N_0}$, the net effect of coupling to the quasicontinuum of excitation modes becomes significant.

A second scenario in which the Bogoliubov approximation is insufficient is that of two macroscopically occupied modes. Consider two excitation modes that are populated with M and N excitations each. In the case of $M,N \approx \sqrt{N_0}$, the depletion of the ground state can still be safely ignored, but the coupling between the two modes is comparable to the interaction between the excitations and the condensate ground state, and therefore should be considered.

The terms of the next lower order in $\sqrt{N_0}$ were first added to the Bogoliubov Hamiltonian by Beliaev in 1958 (Beliaev, 1958). The discussion here will be limited to homogeneous condensates. Collecting those terms in the condensate Hamiltonian that are proportional to $\sqrt{N_0}$, we get the interaction term

$$\hat{H}_{\rm int} = 2\frac{g}{2V}\sqrt{N_0}\sum_{\mathbf{l},\mathbf{m},\mathbf{n}\neq 0}[\hat{a}_{\mathbf{l}}^{\dagger}\hat{a}_{\mathbf{m}}^{\dagger}\hat{a}_{\mathbf{n}} + \hat{a}_{\mathbf{n}}^{\dagger}\hat{a}_{\mathbf{l}}\hat{a}_{\mathbf{m}}]\delta_{\mathbf{l}+\mathbf{m},\mathbf{n}}. \quad (15)$$

All these terms describe atomic collisions between atoms with momenta m,l,n and one ground-state atom.

Changing to the Bogoliubov basis, the interaction Hamiltonian between two excitation modes k and q is (Giorgini, 1998; Rogel-Salazar *et al.*, 2001)

$$\hat{H}_{\rm int} = \frac{g}{2V}\sqrt{N_0}[A_{\mathbf{k},\mathbf{q}}(\hat{b}_{\mathbf{k}-\mathbf{q}}^{\dagger}\hat{b}_{\mathbf{q}}^{\dagger}\hat{b}_{\mathbf{k}} + \hat{b}_{\mathbf{k}}^{\dagger}\hat{b}_{\mathbf{k}-\mathbf{q}}\hat{b}_{\mathbf{q}}) + B_{\mathbf{k},\mathbf{q}}(\hat{b}_{-(\mathbf{k}+\mathbf{q})}^{\dagger}\hat{b}_{\mathbf{q}}^{\dagger}\hat{b}_{\mathbf{k}}^{\dagger} + \hat{b}_{\mathbf{k}}\hat{b}_{-(\mathbf{k}+\mathbf{q})}\hat{b}_{\mathbf{q}})], \quad (16)$$

where

$$A_{\mathbf{k},\mathbf{q}} = 2u_k(u_q u_{|\mathbf{k}-\mathbf{q}|} - u_q v_{|\mathbf{k}-\mathbf{q}|} - v_q u_{|\mathbf{k}-\mathbf{q}|}) - 2v_k(v_q v_{|\mathbf{k}-\mathbf{q}|} - v_q u_{|\mathbf{k}-\mathbf{q}|} - u_q v_{|\mathbf{k}-\mathbf{q}|}), \quad (17)$$

and

$$B_{\mathbf{k},\mathbf{q}} = -2u_k(v_q u_{|\mathbf{k}+\mathbf{q}|} + u_q v_{|\mathbf{k}+\mathbf{q}|} - v_q v_{|\mathbf{k}+\mathbf{q}|}) + 2v_k(u_q v_{|\mathbf{k}+\mathbf{q}|} + v_q u_{|\mathbf{k}+\mathbf{q}|} - u_q u_{|\mathbf{k}+\mathbf{q}|}). \quad (18)$$

There are two types of processes that are described by the above interaction Hamiltonian. The first type, given by the two terms in the first set of parentheses, describes wave-mixing between the different Bogoliubov excitation modes. The first term in the parentheses, $\hat{b}_{\mathbf{k}-\mathbf{q}}^{\dagger}\hat{b}_{\mathbf{q}}^{\dagger}\hat{b}_{\mathbf{k}}$, describes the annihilation of an excitation from mode $\mathbf{k}$ and the creation of two excitations in modes $\mathbf{q}$ and $\mathbf{k}-\mathbf{q}$ in its stead. This process, which is referred to as Beliaev coupling, is analogous to photonic down conversion in optics. The conjugate process (second term in the parentheses) describes the annihilation of two excitations, in modes $\mathbf{q}$ and $\mathbf{k}-\mathbf{q}$, and the creation of an excitation in mode $\mathbf{k}$, which is analogous to optical sum-frequency generation. When thermal excitations are involved, this process is termed Landau damping.

The coupling constant for both of these processes is $A_{k,q}$, which is an interference term between different atomic trajectories for excitation conversion. In the limit of $k\xi,\ q\xi \ll 1, u_{k,q} \approx v_{k,q}$ and therefore $A_{k,q} \approx 0$. This suppression of Beliaev and Landau processes at low momenta is a result of destructive quantum interference. In the limit of $k\xi,\ q\xi \gg 1, v_{k,q} \sim 0$, and $u_{k,q} \sim 1$, and therefore $A_{k,q} \approx 2$.

The second set of parentheses in Eq. (16) describes off-resonance, spontaneous creation or annihilation of three excitations. The first term $\hat{b}_{-(\mathbf{k}+\mathbf{q})}^{\dagger}\hat{b}_{\mathbf{q}}^{\dagger}\hat{b}_{\mathbf{k}}^{\dagger}$ describes the creation of two excitations in modes $\mathbf{q}$ and $\mathbf{k}$ and then the creation of a third excitation in mode $-(\mathbf{k}+\mathbf{q})$ that will carry the added momentum. The second term in the parentheses describes the conjugate process, in which the three excitations are annihilated. $B_{k,q}$, which is again an interference term between different atomic paths, is highly suppressed in both the limits $k\xi, q\xi \ll 1$ and $k\xi, q\xi \gg 1$. These terms describe the spontaneous creation and decay of excitations in an energy nonconserving manner, and are therefore usually overwhelmed by the on-resonance Beliaev and Landau processes (Rogel-Salazar *et al.*, 2001).

For a more elaborate discussion of Beliaev and Landau processes, which is generalized to the cases of nonuniform condensates and nonzero temperature, see Pitaevskii and Stringari (1997), Giorgini (1998), Morgan *et al.* (1998), and Rogel-Salazar *et al.* (2001).

V. TWO-PHOTON BRAGG TRANSITIONS

Two-photon Bragg scattering has been used to impart momentum into different velocity classes of a thermal cloud of laser-cooled atoms (Courtois *et al.*, 1994). In 1999, the group of Phillips at NIST, Maryland used two-photon Bragg transitions to impart momentum into a Bose-condensed cloud of atoms (Kozuma *et al.*, 1999), and to coherently split the cloud in momentum space. Later that year, in two seminal experiments, the group of Ketterle at MIT used two-photon Bragg scattering to excite Bogoliubov excitations in a condensate (Stamper-Kurn *et al.*, 1999; Stenger *et al.*, 1999). The response of the condensate to Bragg transitions of different frequencies provided a spectroscopic measurement of the Bogoliubov excitation energy.

Bragg scattering can be viewed as diffraction of the condensate from a moving optical lattice that is formed by two intersecting laser beams. Atoms diffract from the lattice given that the Bragg condition is fulfilled, i.e., that the energy and momentum imparted to the condensate matches the energy and momentum of the moving optical lattice. The energy of the lattice is determined by the frequency difference between the beams, and the lattice momentum $\hbar\mathbf{k}$ is determined by the beams' angle of intersection.

Given a homogeneous condensate, $\hbar\mathbf{k}$ is a good quantum number. Moreover, since there is a one-to-one correspondence between the excitation momentum and energy, the condensate response is a δ function in the frequency domain [neglecting, for the moment, Eq. (15)]. Currently, realizable condensates are not homogeneous. Consequently, linear momentum is not a good quantum number of the excitations. Nevertheless, the momentum that is being transferred by the Bragg process is well defined. As a result, the relative energetic width that can be excited decreases as k increases. When the wavelength of the perturbation $2\pi/k$ is smaller than the linear size of the condensate, the response of an inhomogeneous condensate resembles that of a homogeneous condensate in many respects.

A. Homogeneous condensates

Bragg scattering can be viewed as Bosonic amplification of photon scattering from a single laser mode, due to a macroscopic photon occupation of the target mode.

Neglecting higher-order photon scattering, the interaction between the atomic ensemble and the laser beams can be written as

$$\hat{H}_B = \frac{\hbar\Omega_B}{2}\sum_{\mathbf{q}} [\hat{a}^\dagger_{\mathbf{q}+\mathbf{k}}\hat{a}_{\mathbf{q}} + \hat{a}_{\mathbf{q}+\mathbf{k}}\hat{a}^\dagger_{\mathbf{q}}]. \tag{19}$$

The dependence of the Hamiltonian on the laser beams and the atom-photon coupling is contained in the Bragg Rabi frequency Ω_B. The operator part of Eq. (19) deals only with the external degrees of freedom of the gas. $\hat{a}^\dagger_{\mathbf{q}}, \hat{a}_{\mathbf{q}}$ are the creation and annihilation operators of free atoms, which are the eigenstates of a noninteracting gas. Therefore each atom in such a gas will perform Rabi oscillations between the momentum states $\mathbf{q}$ and $\mathbf{q}+\mathbf{k}$.

The case of an interacting homogeneous condensate is somewhat more complicated, because a change in the population of an atomic mode changes the interaction energy between atoms. In other words, the free-atom basis, $a^\dagger_{\mathbf{k}}, a_{\mathbf{k}}$, is inadequate and one has to move to the Bogoliubov basis. Collecting terms in Eq. (19) that involve creation or annihilation of an atom in the ground state, and transforming to the Bogoliubov basis, we find

$$\hat{H}_B = \frac{\hbar\Omega_B}{2}\sqrt{N_0}\sqrt{S_k}[\hat{b}_{-\mathbf{k}} + \hat{b}^\dagger_{\mathbf{k}} + \hat{b}^\dagger_{-\mathbf{k}} + \hat{b}_{\mathbf{k}}]. \tag{20}$$

S_k, the static structure factor, is an interference term between different atomic paths to excite the condensate, given by

$$S_k = (u_k - v_k)^2. \tag{21}$$

The Bogoliubov approximation is valid only as long as the excitation population is small compared to that of the ground state. Therefore we cannot use Eq. (20) to describe Rabi oscillations in which the ground state is completely depleted (Katz, Ozeri, Rowen, *et al.*, 2004). Equation (20) is only adequate to describe perturbative evolution. In the perturbative limit it is helpful to use Fermi's golden rule and calculate the rate of excitation via Eq. (20) (Brunello *et al.*, 2001). The rate of excitation from the Bogoliubov vacuum to some mode $\mathbf{q}$ is

$$\Gamma = \frac{2\pi}{\hbar}|\langle 1_{\mathbf{q}}|\hat{H}_B|0\rangle|^2\delta(\hbar\omega - \varepsilon_{\mathbf{q}}). \tag{22}$$

$\hat{H}_B$ contains only two creation operators, one into mode $\mathbf{k}$, and the other into mode $-\mathbf{k}$. Therefore it is only these two modes into which the scattering rate Eq. (22) does not vanish. The scattering rate into mode $\pm\mathbf{k}$ will be

$$\Gamma_{\pm\mathbf{k}} = \frac{2\pi}{\hbar}\frac{(\hbar\Omega_B)^2}{4}N_0 S_{\pm k}\delta(\hbar\omega - \varepsilon_{\pm k}). \tag{23}$$

The two modes will be on resonance at exactly the opposite frequency difference between the beams, the magnitude of which is equal to the Bogoliubov quasiparticle energy, $\varepsilon_k/\hbar$. The above rates are calculated for an initial Bogoliubov vacuum state, but are also independent of any previous population in the excited mode (Brunello *et al.*, 2001; Ketterle and Inouye, 2001).

The rate Eq. (23) can be divided into a factor that depends on the lasers and the single atom-photon coupling, and a factor that depends on the intrinsic properties of the condensate,

$$\Gamma_{\mathbf{k}} = \frac{2\pi}{\hbar}\frac{(\hbar\Omega_B)^2}{4}S(k,\omega). \tag{24}$$

$S(k,\omega) = N_0 S_k \delta(\hbar\omega - \varepsilon_k)$, the factor which depends only on the condensate structure, is called the dynamic structure factor (Brunello *et al.*, 2001; Cohen-Tannoudji and Robilliard, 2001; Ketterle and Inouye, 2001). This quantity has a peak at the quasiparticle energy, which allows for the measurement of the excitation spectrum, as discussed in Sec. VI.A. The measurement of $S(k,w)$ via Bragg scattering is analogous to its measurement by neutron scattering, employed for superfluid ^{4}He, yielding the phonon-maxon-roton excitation spectrum (Nozières and Pines, 1990; Griffin, 1993).

As seen from Eq. (23), the response of the condensate to two-photon Bragg scattering is proportional to S_k. In linear response theory the response of a system to a perturbation with momentum $\hbar\mathbf{k}$ is proportional to density fluctuations with the corresponding wave vector (Plischke and Bergersen, 1994). To relate S_k to the density correlation function, we follow Cohen-Tannoudji and Robilliard (2001) and consider the single-particle density operator,

$$\hat{\rho}(\mathbf{r}) = \hat{\Psi}^\dagger(\mathbf{r})\hat{\Psi}(\mathbf{r}). \tag{25}$$

Expanding into atomic plane waves, $\hat{\rho}(\mathbf{q})$, which is seen to be the Fourier transform of $\hat{\rho}(\mathbf{r})$, is given by

$$\hat{\rho}(\mathbf{q}) = \frac{1}{V}\sum_{\mathbf{k}} \hat{a}^\dagger_{\mathbf{k}+\mathbf{q}}\hat{a}_{\mathbf{k}}. \tag{26}$$

Note that our Bragg Hamiltonian Eq. (19) is composed of $\hat{\rho}(\mathbf{q})$ and its conjugate. In the Bogoliubov basis $\hat{\rho}(\mathbf{q})$ is written as

$$\hat{\rho}(\mathbf{q}) \approx \frac{1}{V}\sqrt{N_0}(\hat{a}_{\mathbf{q}} + \hat{a}_{-\mathbf{q}}) = \frac{1}{V}\sqrt{N_0 S_{\mathbf{q}}}(\hat{b}^\dagger_{\mathbf{q}} + \hat{b}_{-\mathbf{q}}). \tag{27}$$

It is evident from Eq. (27) that the expectation value of $\hat{\rho}(\mathbf{q})^\dagger\hat{\rho}(\mathbf{q})$ with respect to the ground state is proportional to $S_{\mathbf{q}}$, i.e.,

$$\begin{aligned} S_{\mathbf{q}} &= \frac{V^2}{N_0}\langle 0|\hat{\rho}(\mathbf{q})^\dagger\hat{\rho}(\mathbf{q})|0\rangle \\ &= \frac{1}{N_0}\sum_{\mathbf{R}} e^{i\mathbf{q}\cdot\mathbf{R}}\langle 0|\sum_{\mathbf{r}} \hat{\rho}(\mathbf{r}+\mathbf{R})^\dagger\hat{\rho}(\mathbf{r})|0\rangle \\ &= 1 + N_0\sum_{\mathbf{R}} e^{i\mathbf{q}\cdot\mathbf{R}}[g(\mathbf{R}) - 1], \end{aligned} \tag{28}$$

where $g(\mathbf{R})$ is the ground-state pair-correlation function giving the conditional probability to find two atoms separated by a displacement $\mathbf{R}$. For a homogeneous condensate $g(R)$ is isotropic and only depends on R, the magnitude of $\mathbf{R}$.

Let us now look at the behavior of S_k as a function of k. Inserting Eq. (7) into Eq. (21), we find

$$S_k = u_k^2 + v_k^2 - 2u_k v_k = \frac{\epsilon_k^0}{\epsilon_k}. \tag{29}$$

This relation between the excitation spectrum and the condensate spectral response is known as the Feynman-Bijl relation, and is the result of the *f*-sum rule in linear response theory (Brunello *et al.*, 2001). It is a striking result, in which the complete excitation spectrum can be extracted from an expectation value taken with respect to the ground state only.

The relation Eq. (29) was experimentally verified by the MIT group using Bragg spectroscopy, as shown in Fig. 3. As ϵ_k increases in Fig. 3(b), S_k is seen to decrease in Fig. 3(a). Since the condensate in the experiment was inhomogeneous, the solid curve of Fig. 3(a) gives the result of the local density approximation (see Sec. V.C).

Using the definition of the healing length, we can rewrite Eq. (29) as

$$S_k = \frac{(k\xi)^2}{\sqrt{(k\xi)^4 + 2(k\xi)^2}}. \tag{30}$$

The response of the condensate at different momenta is now clear. For excitations in the single-particle regime, $k > \xi^{-1}$ and $S_k \simeq 1$, as one would expect for a gas of atoms where interatomic distances are not correlated. For excitations in the phonon regime, $k < \xi^{-1}$ and $S_k \simeq k\xi/\sqrt{2}$. Thus the response of the condensate decreases linearly with k. The decrease of the condensate response at low momenta is a quantum interference effect, in which atoms that, owing to interactions, are removed from the $k=0$ mode, are moving in opposite directions, and conspire to suppress oscillations in $g(r)$. Within the mean-field framework, S_k never exceeds unity, which implies that there is no "typical" interatomic distance in the condensate, consistent with the dilute gas assumption. This is in contrast to superfluid ^{4}He, which has a peak in S_k corresponding to the roton, reflecting short-range correlations due to the liquid nature of superfluid ^{4}He (Griffin, 1993).

B. Trapped condensates

Although linear momentum is not a quantum number describing excitations in trapped condensates, the response of the condensate to the Bragg pulse is typically measured through the efficiency of momentum transfer. There have been several quantum-mechanical treatments evaluating the momentum transfer to a trapped condensate (Brunello *et al.*, 2001; Blakie *et al.*, 2002). Here we will describe one of these methods, the evolution of Eq. (11) under the Bragg potential (Brunello *et al.*, 2001; Band and Sokuler, 2002; Blakie *et al.*, 2002; Tozzo and Dalfovo, 2003). Due to its simplicity and accuracy, this method is the most common in analyzing the outcome of Bragg experiments.

One view of Bragg scattering is diffraction of a matter wave from a moving optical lattice potential, formed by the two Bragg beams,

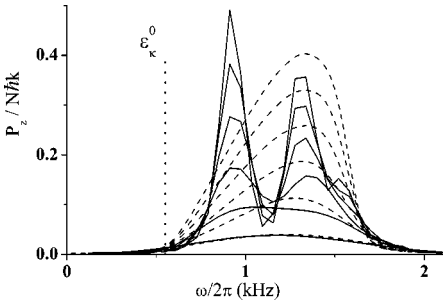

FIG. 4. The condensate response to the Bragg pulse, calculated from a Gross-Pitaevski simulation, performed at the Universita Cattolica del Sacro Cuore, Brescia, Italy, by C. Tozzo and F. Dalfovo. The simulation was done for the experimental parameters of Steinhauer *et al.* (2003), at $k\xi=0.74$ (solid lines). Momentum was imparted along the axial direction of the elongated condensate. Different curves, with increasing multipeaked structure, correspond to Bragg pulses of different duration, 1, 2, 3, 4, 5, and 6 msec. These curves are compared with the local-density approximation (LDA) average (dashed curves) from Eq. (41). From Steinhauer *et al.*, 2003.

$$V_{\text{Bragg}} = \theta(t)\frac{\hbar\Omega_B}{2}\cos(kz - \omega t), \tag{31}$$

where z is chosen to be in the direction of the wave-vector difference between the beams, $\mathbf{k}$. $\theta(t)$ is a step function that describes a sudden turn-on and a sudden turn-off of the Bragg beams.

In order to solve for the evolution of the condensate wave function in the presence of V_{Bragg}, it is possible to numerically evolve Eq. (11) in time (Brunello *et al.*, 2001). The momentum transferred to the condensate after time t can be calculated directly from the solution $\phi(\mathbf{r},t)$,

$$P_z(t) = \frac{-i\hbar}{2}\int [\phi^*(\mathbf{r},t)\nabla_z\phi(\mathbf{r},t) + \text{c.c.}]d\mathbf{r}. \tag{32}$$

Within the mean-field assumptions this is a full simulation of the Bragg scattering experiment.

Figure 4 (solid lines) shows the thus calculated response of the condensate. The simulation solves Eq. (11) with the Bragg potential for the experimental parameters of Steinhauer *et al.* (2003), at $k\xi=0.74$. Momentum is imparted along the axial direction of the elongated condensate. It is seen that for sufficiently short pulses, the response has a single resonance, which is shifted from the free atom energy ϵ_k^0, indicated by the dotted line. Conversely, for longer pulses, the Gross-Pitaevski simulations show a splitting of the resonance into a multipeak structure.

This multipeak structure is due to different excitation spectra, each belonging to an axial quasiparticle, in a different radial mode, corresponding to Eq. (14) (Steinhauer *et al.*, 2003; Tozzo and Dalfovo, 2003). The large aspect ratio of the condensate enables momentum transfer along the axial dimension to be almost continuous, while different radial modes are still well resolved.

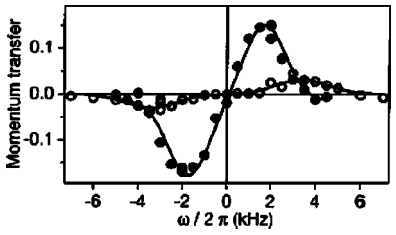

FIG. 5. The normalized transferred momentum $P(k,\omega)$. The filled and open circles are for trapped ($k\xi=0.57$) and released (low-density) condensates, respectively. The lines are fits of the difference of two Gaussians. From Stamper-Kurn *et al.*, 1999.

C. Local-density approximation and Doppler broadening

It is often useful to have an approximation that gives an analytic form to $S(k,\omega)$, the condensate response to the Bragg pulse. Such an approximation exists in the limit $k^{-1}\ll R_{\mathrm{TF}}$, in which case the change in density over the excitation wavelength is small. The condensate can then be treated as an ensemble of homogeneous condensates, each of which has its own density, local energy spectrum, and response function (Stamper-Kurn *et al.*, 1999; Zambelli *et al.*, 2000). This is called the local-density approximation (LDA). The Bogoliubov energy at the point $\mathbf{r}$, is then given by $\epsilon_k(\mathbf{r})=\sqrt{\epsilon_k^0[\epsilon_k^0+2n(\mathbf{r})g]}$.

For a condensate trapped in an harmonic potential, in the Thomas-Fermi approximation, the dynamic structure factor in the LDA is given by (Stamper-Kurn *et al.*, 1999; Zambelli *et al.*, 2000)

$$S(k,\omega)=\frac{15}{8}\frac{[(\hbar\omega)^2-\epsilon_k^{02}]}{\epsilon_k^0\mu^2}\sqrt{1-\frac{[(\hbar\omega)^2-\epsilon_k^{02}]}{2\epsilon_k^0\mu}}. \tag{33}$$

S_k is consequently given by (Stamper-Kurn *et al.*, 1999; Zambelli *et al.*, 2000)

$$S_k=\frac{15}{4}\left\{\frac{3+\alpha}{4\alpha^2}-\frac{3+2\alpha-\alpha^2}{16\alpha^{5/2}}\times\left[\pi+2\arctan\left(\frac{\alpha-1}{2\sqrt{\alpha}}\right)\right]\right\}, \tag{34}$$

where $\alpha=2\mu/\epsilon_k^0$. ϵ_k is then given by the Feynman-Bijl relation [Eq. (29)], which survives the LDA averaging.

In the phonon regime ($k\xi<1$), the Bogoliubov energy can be approximated by

$$\epsilon_k\simeq c_{\mathrm{eff}}k, \tag{35}$$

where

$$c_{\mathrm{eff}}\equiv\frac{32}{15\pi}\sqrt{\frac{\mu}{m}} \tag{36}$$

is the speed of sound averaged in the LDA. As expected, it is lower than the speed of sound in the center of the condensate. The excitation energy Eq. (35) is well above the free particle energy ϵ_k^0, as was observed experimentally by the MIT group, as shown in Fig. 5. The peak indicated by filled circles is located at a frequency close to ϵ_k^0/h, whereas the peak indicated by open circles is located at ϵ_k/h.

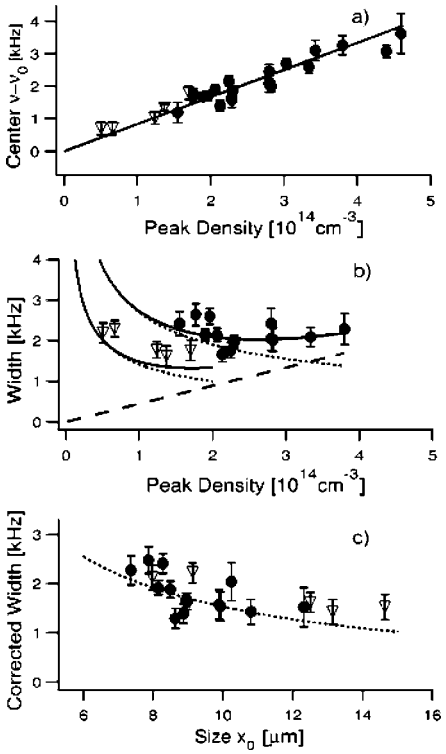

FIG. 6. Measurements in the single-particle regime with a k value corresponding to $\epsilon_k^0=h\times 100$ kHz. The data were taken with two different trap radial frequencies, $\omega_\rho=2\pi\times 195$ Hz (circles) and $\omega_\rho=2\pi\times 95$ Hz (triangles): (a) the linear dependence on density of Eq. (37); (b) the total width (solid curve), which is the quadrature sum of the LDA width of Eq. (40) (dashed curve) and the Doppler width of Eq. (42) (dotted curve); (c) the width after subtraction of the calculated LDA and finite-time contributions (leaving Doppler broadening contribution only). From Stenger *et al.*, 1999.

In the single-particle regime $k\xi>1$, the Bogoliubov energy can be written as

$$\epsilon_k\simeq\epsilon_k^0+\frac{4}{7}\mu. \tag{37}$$

ϵ_k thus has the same form as in the homogeneous case, where the mean-field shift corresponds to the value of the shift at the average density, $4n/7$. This linear dependence of ϵ_k on $\mu=gn$ was verified experimentally by Stenger *et al.* (1999), as shown in Fig. 6(a).

Recalling Fig. 1, we note that the LDA average (dotted line) and the appropriate homogeneous condensate excitation spectrum are nearly overlapping. This similarity reflects the fact that, for large momentum transfer, the response of the condensate is dominated by its "bulk" properties rather than its geometry.

The LDA can also be used to compute the frequency width of the condensate response $S(k,\omega)$,

$$\hbar\Delta\omega_{\mathrm{LDA}} = \sqrt{\langle\epsilon_k(\mathbf{r})^2\rangle_{\mathrm{LDA}} - \epsilon_k^2}$$
$$= \sqrt{\frac{1}{N_0 S_k}\int \epsilon_k(\mathbf{r})^2 n(\mathbf{r})\frac{\epsilon_k^0}{\epsilon_k(\mathbf{r})}d\mathbf{r} - \epsilon_k^2}$$
$$= \sqrt{\epsilon_k(\langle\epsilon_k(\mathbf{r})\rangle - \epsilon_k)}, \tag{38}$$

where $\langle\epsilon_k(\mathbf{r})\rangle = (1/N_0)\int \epsilon_k(\mathbf{r})n(\mathbf{r})d\mathbf{r}$, is the normal averaging of $\epsilon_k(\mathbf{r})$ over the condensate volume (without taking the local response into account).

For an external harmonic trapping potential, in the phonon regime, the width of the response is given by (Zambelli *et al.*, 2000)

$$\Delta\omega_{\mathrm{LDA}} \simeq 0.3 c_{\mathrm{eff}} k \simeq 0.3\frac{\epsilon_k}{\hbar}. \tag{39}$$

In this part of the spectrum, dephasing will occur on almost the same time scale as the phonon oscillation period.

In the single-particle regime, the width of the response is independent of k, and given by (Zambelli *et al.*, 2000)

$$\Delta\omega_{\mathrm{LDA}} \simeq \sqrt{\frac{8}{147}}\frac{\mu}{\hbar}. \tag{40}$$

This relation is indicated by the dashed line in Fig. 6(b). In this figure, the measured width of the line in the single-particle regime was seen to be consistent with the quadrature sum of Eq. (40), with the Doppler width given in Eq. (42). For elongated traps, the inhomogeneous frequency broadening can be largely suppressed using a Bogoliubov Bragg-echo technique (Gershnabel, Katz, Ozeri, *et al.*, 2004).

In order to compare the LDA predictions with the results of the more accurate Gross-Pitaevski simulations, the finite time of the Bragg pulse must be incorporated into the LDA theory. The condensate response to the Bragg pulse is given by the convolution of the pulse's normalized spectral content with the intrinsic response of the condensate in the LDA (Brunello *et al.*, 2001),

$$P(k,\omega) = \frac{1}{\pi}\int S(k,\omega')\frac{\sin[(\omega-\omega')t_B]}{\omega-\omega'}d\omega'. \tag{41}$$

Figure 4 compares the calculated response of the condensate using Gross-Pitaevski simulations and the LDA approximation (Steinhauer *et al.*, 2003). The solid lines are the result of Gross-Pitaevski simulations, and the dashed lines are the result of Eq. (41). It is seen that for sufficiently short pulses, the response predicted by the Gross-Pitaevski equation is in good agreement with the LDA predictions. However, for pulses longer than $t_B \simeq 2\pi/\omega_\rho$, where ω_ρ is the radial oscillation frequency of the trap, the Gross-Pitaevski results and the LDA predictions greatly disagree. As opposed to the LDA's single resonance peak, the Gross-Pitaevski simulations show a splitting into various radial modes.

The LDA cannot possibly predict the radial mode structure in the condensate response, as it ignores the condensate's geometry. However, the LDA is found to succeed in indicating which of the radial modes will be excited. Only radial modes with energies within the LDA peak are excited (Tozzo and Dalfovo, 2003).

Given that the Bragg potential has no radial dependence, it will only act on axial degrees of freedom. Hence radial modes will be excited in proportion to the overlap integral of the radial part of the excitation wave function, with the radial part of the ground-state wave function (Tozzo and Dalfovo, 2003). In this respect, the two conditions (LDA and overlap integral) are in very good agreement. This agreement persists also for anharmonic trap geometries, where the LDA and the overlap integrals both predict the excitations of a single or very few radial modes, due to the much smaller inhomogeneity (Gershnabel, Katz, Rowen, *et al.*, 2004).

In addition to the inhomogeneous density, the finite size of the condensate is a source of broadening of the response to the Bragg pulse. The finite size is translated into a finite-width momentum distribution. The resulting broadening is called Doppler broadening (Stenger *et al.*, 1999).

The Doppler width is evaluated by explicitly integrating over the ground-state momentum distribution for a trapped condensate in the Thomas-Fermi limit as (Stenger *et al.*, 1999; Zambelli *et al.*, 2000)

$$\Delta\omega_D = \sqrt{\frac{8}{3}}\frac{v_r}{R_{\mathrm{TF}}}, \tag{42}$$

where the recoil velocity v_r is given by $\hbar k/m$. This Doppler width was seen to agree well with the measured broadening of the response to the Bragg pulse, as shown in Fig. 6(c) (Stenger *et al.*, 1999).

In the time domain, dephasing will occur on a time scale of R_{TF}/v_r. This is also the time required for the excitations to reach the edge of the condensate. This is a manifestation of the fact that the coherence length of the condensate is equal to its size. In fact, the opposite point of view can be adopted, that the measurement of the Bragg Doppler width can be viewed as a measurement of the condensate coherence length. An experiment at MIT showed that the coherence length is indeed approximately equal to the condensate size (Stenger *et al.*, 1999). Experiments by the group of A. Aspect at Orsay measured the coherence length of one-dimensional quasicondensates (Richard *et al.*, 2003).

VI. COHERENT EXCITATION EVOLUTION

Two experimental approaches are presented for measuring the excitation spectrum of a condensate. The first is Bragg spectroscopy (Stamper-Kurn *et al.*, 1999; Stenger *et al.*, 1999; Steinhauer *et al.*, 2002, 2003). In the second approach, the spectrum is measured by monitoring the time evolution of the Bragg excited condensate (Ozeri *et al.*, 2002).

The dynamics that are probed in these experiments are governed by the Bogoliubov Hamiltonian, and are therefore coherent and time reversible. Even the excita-

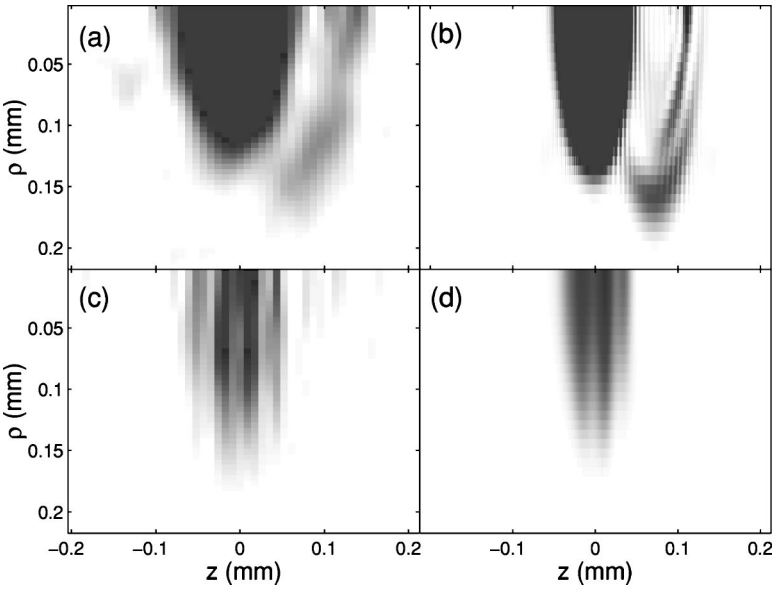

FIG. 7. Radial and axial density profiles of the released, excited condensate after 38 msec of flight. The profiles are generated by computerized tomography of the absorption images (see VI.B). The excitations' momenta correspond to (a) $k\xi=0.67$ and (c) $k\xi=0.1$. For the lowest momentum value (c), the released excitations form fringes in the released condensate. For (a) the condensate and the released excitations form two fairly distinct clouds. (b) and (d) are the result of a full Gross-Pitaevskii equation simulation with the same experimental parameters as in (a) and (c), respectively. From Katz, Ozeri, Steinhauer, *et al.*, 2004.

tions' dephasing in time is caused by inhomogeneity in the condensate, and can therefore be time reversed, by the use of echo techniques, for example.

A. Frequency domain—Measurement of the Bogoliubov spectrum

In order to directly measure the excitation spectrum the following experimental procedure is employed. The Bragg beams are directed at the condensate at a fixed intersection angle. This angle determines the momentum transfer of a single Bragg scattering event,

$$\hbar k = 2\hbar k_L \sin(\theta/2), \tag{43}$$

where $2\pi/k_L$ is the Bragg laser wavelength. For each angle of intersection, the Bragg beams are pulsed for a time t_B, and the condensate response to the pulse is measured. The experiment is repeated for various ω, the frequency difference between the beams. The response of the condensate to the Bragg pulse, as a function of ω, is determined by $S(k,\omega)$, the dynamic structure factor. The Bogoliubov excitation energy ϵ_k is defined as the energy averaged over $S(k,\omega)$ (Stamper-Kurn *et al.*, 1999; Stenger *et al.*, 1999; Zambelli *et al.*, 2000; Steinhauer *et al.*, 2002).

The wave vector **k** is adjusted to be in the axial direction z of the cigar-shaped condensate. This way the wavelength of the excitations will be much smaller than the condensate size, for a wide range of wavelengths.

After the Bragg pulse, the atoms are allowed to expand freely, transforming the excitations into free particles. After a certain time of flight (TOF), the atomic cloud is imaged by an on-resonance absorption beam. Figures 7(a) and 7(c) show a radial and axial density profile generated by computerized tomography (see Sec. VI.B) of the TOF absorption images of Rb condensates excited with excitations of $k\xi=0.67$ and 0.1, respectively. The left and right clouds correspond to the condensate and released excitations, respectively.

For the very lowest momentum excitations, such as $k\xi=0.1$, where the excitation energy is smaller than $\hbar\omega_\rho$, the released excitations form a fringe pattern in the expanding condensate (Katz, Ozeri, Steinhauer, *et al.*, 2004; Tozzo and Dalfovo, 2004). At such low momentum, the velocity of the excitations after changing to free particles during the condensate expansion, is less than the residual axial expansion velocity of the condensate. Consequently, the excitations never leave the condensate bulk, and form a matter-wave interference pattern. This method of observing excitations via measurement of matter-wave fringe visibility is remarkably sensitive, since the condensate acts as a local heterodyne oscillator for the traveling excitation atoms. However, the interference pattern is only observed at very low excitation momentum, and therefore the momentum counting method described below is more generally used. For higher Bragg momentum values, the condensate and the released excitations form two fairly distinct clouds. Figures 7(b) and 7(d) are Gross-Pitaevski simulations of Figs. 7(a) and 7(c), respectively.

To determine the momentum that is transferred by the Bragg pulse, the total momentum in the axial direction relative to the center of the condensate cloud is computed from the image, in the combined regions of the two clouds. In the TOF image, an atom's position is proportional to its momentum. The absorption picture provides $n(x,y,z)$ integrated along the absorption beam axis, $f(y,z)=\int n(x,y,z)dx$. The momentum of the atomic cloud is calculated as

$$p(k,w) = \frac{m}{\tau}\int z f(y,z)dydz, \tag{44}$$

where τ is the time of flight.

The pulse normalized transferred momentum $P(k,\omega)$ is given by the momentum that was transferred to the condensate, counted in units of $\hbar k$ (number of excitations formed) divided by N_o, the average number of atoms in the condensate during the Bragg pulse,

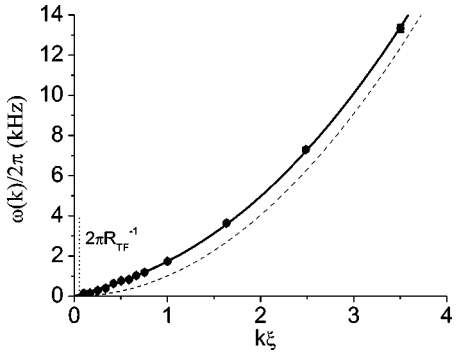

FIG. 8. The measured excitation spectrum $\omega(k)$ of a trapped Bose-Einstein condensate (filled circles): solid curve, the Bogoliubov spectrum with no free parameters, in the LDA for $\mu=1.91$ kHz; dashed curve, the parabolic free-particle spectrum. For most points, the error bars are not visible on the scale of the figure. From Steinhauer *et al.*, 2002.

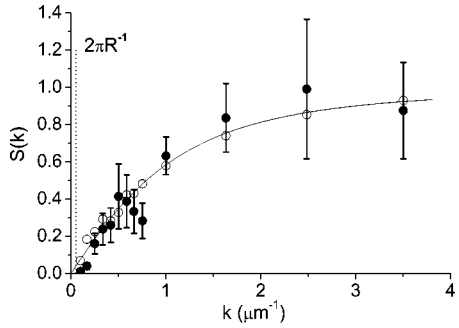

FIG. 9. The measured static structure factor and Bogoliubov structure factor. The filled circles are the measured static structure factor, multiplied by an overall constant of 2.3 (Steinhauer *et al.*, 2002). Error bars represent 1σ statistical uncertainty, as well as the estimated uncertainty in the two-photon Rabi frequency. The solid line is the Bogoliubov structure factor in the LDA for $\mu=1.91$ kHz. The open circles are computed from the measured excitation spectrum of Fig. 8 and the Feynman-Bijl relation, Eq. (29). For the open circles, the error bars are not visible on the scale of the figure. From Steinhauer *et al.*, 2002.

$$P(k,\omega)=\frac{p(k,\omega)}{N_o\hbar k}. \tag{45}$$

The thus-measured $P(k,\omega)$ is indicated in Fig. 5 by open circles, for $k\xi=0.57$. $P(k,\omega)$ is seen to be well approximated by the difference of two Gaussians. The Bogoliubov frequency is given by the average frequency of $S(k,\omega)$. The resonance frequency is therefore taken as the center value of one of the Gaussians from the fit to $p(k,\omega)$.

The density dependence of the Bogoliubov frequency, both in the phonon regime and in the free-particle regime, were measured in two MIT experiments. The results of these experiments are shown in Figs. 3(b) and 6(a), respectively. The solid line in both figures is given by Eq. (8) averaged in the LDA. As predicted by Eq. (8) the quasiparticle energy is seen to increase with the chemical potential, $\mu=gn$.

Figure 8 shows the measured excitation spectrum. The filled circles are the measured resonance frequencies, the solid curve is the LDA averaged Bogoliubov spectrum, using an independently measured value for μ, and without any free parameters. The dashed curve indicates the free-particle parabola. The measured spectrum shows a linear phonon regime for low k, and a parabolic single-particle regime for high k. The excitations seen to have the smallest value of ω/k are the phonons. Therefore, by the Landau criterion, the superfluid critical velocity v_c is bounded by ω/k for the phonons.

A fit to the lower momentum part of the measured spectrum gives the speed of sound for the condensate to be $c_{\text{eff}}=2.0\pm0.1$ mm sec^{-1}, which is also the measured upper bound for v_c. This value is in good agreement with the theoretical LDA value of 2.01 ± 0.05 mm sec^{-1} from Eq. (36). The line at $2\pi R_{\text{TF}}^{-1}$ indicates the excitation whose wavelength is equal to the Thomas-Fermi radius of the condensate in the axial direction. The measured $\omega(k)$ agrees with the LDA, even for k values approaching this lower limit of the region of validity.

Since the spectral content of the pulse in Eq. (41) is normalized, the integral of $P(k,\omega)$ over ω is equal to the integral of $S(k,\omega)$. $S(k)$ is therefore given by

$$S(k)=2(\pi\Omega_B^2 t_B)^{-1}\int P(k,\omega)d\omega. \tag{46}$$

All of the dependence on the Bragg beam parameters is contained in the factors before the integral in Eq. (46). Therefore, by using the same Bragg pulse for every measurement, the integral in Eq. (46) can be used to make relative measurements of $S(k)$. In this way, the suppression of the response in the phonon regime was observed in an MIT experiment, as shown in Fig. 5. The area of the peak indicated by filled circles is proportional to $S(k)$, for atoms that are approximately free (low density). The area of the peak indicated by open circles is proportional to $S(k)$ in the phonon regime (high density). The thus-measured $S(k)$ as a function of density is shown in Fig. 3(a).

The filled circles in Fig. 9 are the measured values of the static structure factor $S(k)$, plotted vs k, given by Eq. (46). The values shown have been increased by a factor of 2.3 to give rough agreement with the LDA expression, Eq. (34), which is indicated by a solid line. The required factor of 2.3 probably reflects inaccuracies in the various experimental values needed to compute Ω_R. The open circles are computed from the Feynman-Bijl relation, Eq. (29), using the measured values of $\omega(k)$ shown in Fig. 8.

For large k (short wavelength), $S(k)$ approaches unity, corresponding to noninteracting, uncorrelated atoms. Since $S(k)$ is always less than unity for the values of k measured here, the density fluctuations are never greater than in the uncorrelated case, thus confirming the condensate's gaseous nature.

In the measurements of Figs. 8 and 9, the time duration of the pulse was chosen such that the spectral con-

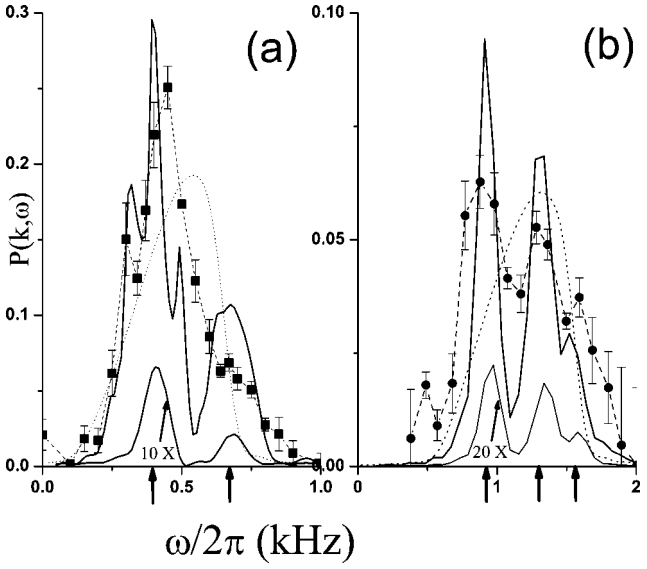

FIG. 10. The response of the condensate to long Bragg pulses (Steinhauer *et al.*, 2003): (a) $k\xi=0.34$ and $\tau_B=10$ msec; (b) $k\xi=0.74$ and $\tau_B=6$ msec. The measured values are indicated by filled circles. Solid curves, the result of Gross-Pitaevskii simulations with various Bragg beam strengths (note that the smaller curves, corresponding to weaker pulses, have been multiplied by a factor, indicated in the figure, in order to fit to the figure scale); dotted curves, the LDA predictions; dashed curves are guides to the eye. From Steinhauer *et al.*, 2003.

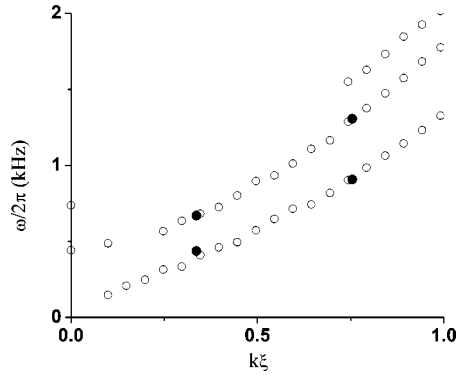

FIG. 11. Excitation frequencies vs k for a trapped, elongated BEC: open circles, the frequencies of the normal modes with $n=0,1,2,\ldots$ nodes in the radial direction, as calculated from the Gross-Pitaevskii equation; filled circles, the positions of the maxima of the main peaks in the measured values of Fig. 10. From Steinhauer *et al.*, 2003.

tent of the pulse was larger than the intrinsic resonance width. In order to resolve the intrinsic line shape of the resonance, longer Bragg pulses are needed.

Figures 10(a) and 10(b) show Bragg spectra for $k\xi=0.74$ and 0.34, respectively, and pulse durations of 6 and 10 msec, respectively. The spectral content of the pulses is therefore smaller than ω_ρ and narrower than $\Delta\omega_{\mathrm{LDA}}$ [Eq. (40)], which are calculated to be $2\pi\times220$ Hz and $2\pi\times446$ Hz for Figs. 10(a) and 10(b), respectively. The filled circles are the measured response. The errors on these points come from the statistical spread of data at every frequency bin. The solid lines are the results of a Gross-Pitaevski simulation. The dotted lines are the LDA predictions of Eq. (41). The measured points are in better agreement with the multi-peak structure of the Gross-Pitaevski simulation than with the LDA curve.

The measured peaks of Fig. 10 are broader than those of the Gross-Pitaevski simulation. This is probably due to frequency noise in the measurement. The major source of such noise is estimated to be random sloshing of the condensate during the Bragg pulse, which produces a Doppler shift. The width of the peaks in the Gross-Pitaevski simulation is determined by the finite duration of the pulse, and for long enough pulses is limited by the density inhomogeneity along the axial direction.

The two solid lines for each of Figs. 10(a) and 10(b) indicate Gross-Pitaevski simulations of different Bragg beam strengths. Although some additional small features are apparent in the strong Bragg simulation, the overall shape of the resonance is very similar for both strengths. Thus nonlinear effects play a small role in the observed multipeak structure. When much stronger Bragg pulses are applied, the observed spectrum is modified significantly due to nonlinear effects (Band and Sokuler, 2002; Katz, Ozeri, Rowen, *et al.*, 2004).

To further support the observation that each of the peaks in Fig. 10 correspond to different radial modes, the oscillations induced by the Bragg pulse in the Gross-Pitaevski simulation are analyzed. After a short Bragg pulse the condensate is allowed to freely oscillate, and density variations in time are Fourier analyzed. This analysis shows that for every k, the density oscillates in a superposition of modes $\omega_n(k)$. The observed frequencies are indicated by arrows along the frequency axis of Figs. 10(a) and 10(b), and are seen to coincide with the peaks of the response.

The open circles of Fig. 11 show the thus-calculated mode frequencies as a function of k. The measured resonance frequencies, which are extracted from fits to the peaks of the measured data of Fig. 10, are indicated by filled circles, and are seen to be in good agreement with the Gross-Pitaevski calculation.

For the case of an infinite homogeneous cylindrical condensate, it can be directly shown that the dynamic structure factor consists of δ functions at the radial mode frequencies (Tozzo and Dalfovo, 2003).

B. Time domain—Direct observation of the phonon energy

The spectral response of the condensate is directly related to the time evolution of excitations. To directly measure the phase evolution and dephasing of excitations, one would have to use interferometric methods. Ramsey and Rabi Bragg interferometry have been applied to BECs in several experiments (Hagley *et al.*, 1999; Simsarian *et al.*, 1999; Torii *et al.*, 2000; Katz, Ozeri, Rowen, *et al.*, 2004). However, in all of these experiments large fractions of the condensate were excited, and therefore the time dynamics did not correspond to

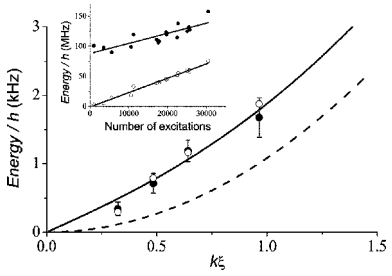

FIG. 12. Excitation energies measured from absorption images at different momenta: filled circles, the slope of the filled circles of the inset, measured in the combined region of the two clouds; open circles, the slope of the open circles in the inset, measured in the region of the excitation cloud only; solid line, the Bogoliubov dispersion relation, calculated in the LDA; dashed curve, the free-particle spectrum. The inset shows the measured energies of the clouds as a function of the number of excitations, for $k\xi=0.96$. The solid lines in the inset are linear fits. From Ozeri *et al.*, 2002.

that of Bogoliubov excitations. An alternative approach would be to measure the excitation energy in the time domain, using kinematic observations (Ozeri *et al.*, 2002).

In Fig. 8, the measured $\omega(k)$ is clearly above the parabolic free-particle spectrum $\hbar k^2/(2m)$. This energy shift consists mainly of interaction energy between the excitations and the condensate. When the trapping potential is turned off, all the interaction energy is transformed into kinetic energy during a short acceleration period. The energy of a single excitation can therefore be extracted from the kinetic energy measurement of an excited condensate, after release.

The absorption picture provides $n(x,y,z)$ integrated along the absorption beam axis, which is sufficient in order to measure the cloud momentum in the z direction. On the other hand, the measurement of the cloud's kinetic energy requires the knowledge of the momentum components in three dimensions. Consequently, the full $n(x,y,z)$ is needed. In general, computerized tomography (CT) can be used in order to reconstruct $n(x,y,z)$ from its Radon projections. Since the cloud is cylindrically symmetric, $n(\rho,z)$ can be CT reconstructed from a single absorption image (Ozeri *et al.*, 2002). Figure 7(a) shows the reconstructed $n(\rho,z)$ for $k\xi=0.67$. The condensate cloud and the released excitation cloud are distinct and separate. The right cloud is clearly larger in the radial direction than the left cloud, reflecting the interaction energy of the excitations.

The filled circles in the inset of Fig. 12 are the measured energy of the atoms in both clouds as a function of the measured number of excitations for $k\xi=0.96$. The slope of these points is $E_k/h=1675\pm290$ Hz and corresponds to the energy of a single excitation. This energy is in agreement with $E_k/h=1780$ Hz, calculated from the Bogoliubov dispersion relation averaged in the LDA. Figure 12 shows the excitation energies measured this way, at four different momenta. The measured energies agree with the LDA averaged Bogoliubov spectrum, indicated by the solid curve.

The open circles in the inset of Fig. 12 are the measured energy in the released excitation cloud only, as a function of the measured number of excitations. The slope of a linear fit to these points is 2390 ± 90 Hz. When the average energy of an atom in the condensate cloud is subtracted from this value, we find an energy of 1840 ± 100 Hz per excitation in the released excitation cloud, which is consistent with the Bogoliubov value $E_k/h=1780$ Hz. This indicates that all of the excitation energy is indeed carried by the atoms in the released excitation cloud. A full Gross-Pitaevski simulation of the excitation and expansion dynamics, as shown in Fig. 7(b), confirms this result (Katz, Ozeri, Steinhauer, *et al.*, 2004).

Each of the filled circles in Fig. 12 is the excitation energy measured from the slope of the energy of the released excitation cloud versus the number of excitations (inset of Fig. 12). Except for the $k\xi=0.32$ point, the measured points agree with the Bogoliubov spectrum in the LDA, indicated by the solid curve.

VII. INCOHERENT EXCITATION EVOLUTION

The Bogoliubov Hamiltonian consists of atomic processes such as forward scattering, which do not change the occupation of different atomic momentum modes, but rather give rise to a phase shift in the atomic wave function. In the Bogoliubov quasiparticle basis, these phase shifts are manifested in the Bogoliubov quasiparticle energy. The evolution of excitations under this Hamiltonian is coherent.

When taken to the next order in $\sqrt{N_0}$, in Eq. (15), the interaction Hamiltonian includes processes for which the occupation of different momentum modes changes. In the large momentum regime, these processes describe an elastic collision between an excitation atom and an atom in the ground state. In the low k regime, these processes are more conveniently described in the Bogoliubov basis, as the decay of an excitation into two lower energy excitations. For typical k values in Bragg scattering experiments, the set of modes to which an excitation can couple form a quasicontinuum in momentum space. The excitation evolution under a Hamiltonian, that couples into a quasicontinuum of modes is incoherent. Scattering of excitations causes an exponential decrease in the mode population and the excitation phase to decohere in a manner that is effectively not time reversible. In the frequency domain, this decoherence leads to a broadening of the Bragg line, which is in a sense the excitation's "intrinsic" linewidth. This broadening is not caused by the inhomogeneity of the condensate, and cannot be overcome by modern spectroscopic techniques, such as echo spectroscopy.

A. Time domain—Suppression of collisional damping at low *k*

In typical absorption images for $k\xi\gg1$, a clear spherical halo of collisional, or Beliaev damping, products is

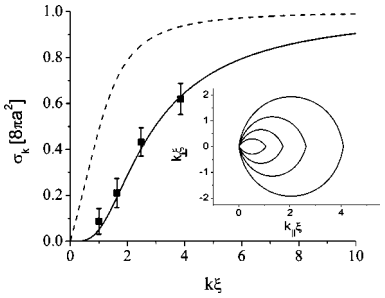

FIG. 13. Cross section for Beliaev damping as a function of $k\xi$, the excitation momentum: solid line, calculated in the LDA; dashed line, calculated without the contribution of $A_{k,q}$, the many-body suppression factor. The experimental points from Katz *et al.* (2002) show the measured cross section (scaled from arbitrary units). The inset shows the energy- and momentum-conserving surfaces for the Bogoliubov dispersion. The $k_\parallel$ and $k_\perp$ axes correspond to the parallel and orthogonal components of the scattered momentum $\mathbf{k}$, respectively. The manifolds are calculated for the experimental values of $k\xi$=3.87, 2.49, 1.63, and 1 (outermost to innermost).

apparent between the condensate and the released excitation clouds. The two clouds are at the poles of a collisional sphere. However, at lower $k\xi$ such as in Fig. 7(a), distinguishing the scattered atoms from the coherent evolution becomes difficult.

The damping rate of N excitations in mode k is calculated from the Beliaev Hamiltonian (16), by the use of Fermi's golden rule (Sakurai, 1985; Ketterle and Inouye, 2001),

$$\Gamma = \frac{2\pi}{\hbar}\sum_{\mathbf{q}'} |\langle (N-1)_{\mathbf{k}}, 1_{\mathbf{q}'}|\hat{H}_{\rm int}|N_{\mathbf{k}}, 0_{\mathbf{q}'}\rangle|^2 \delta(\epsilon_{\mathbf{k}} - \epsilon_{\mathbf{q}'} - \epsilon_{\mathbf{k}-\mathbf{q}'}). \tag{47}$$

The energies in the δ function are the Bogoliubov quasiparticle energies. The off-resonance terms in $\hat{H}_{\rm int}$, which are proportional to $B_{k,q'}$, are thus neglected. At zero temperature there is no initial occupation in the modes $\mathbf{q}'$, and therefore Landau damping processes do not occur. We consider the case for which the time of our experiment $t_{\rm eff}$, is such that

$$\Gamma t_{\rm eff} \ll N_{\rm mode}, \tag{48}$$

where $N_{\rm mode}$ is the number of modes $\mathbf{q}'$ that fulfil the energy-conservation δ-function condition. This way, the average number of excitations scattered into mode $\mathbf{q}'$ throughout the experiment is smaller than 1. We can therefore concentrate on the Beliaev term in the interaction Hamiltonian. The damping rate becomes

$$\Gamma = \frac{2\pi}{\hbar}\frac{g^2 N_0 N}{2V^2}\sum_{\mathbf{q}'} |A_{\mathbf{k}}, \mathbf{q}'|^2 \delta(\epsilon_{\mathbf{k}} - \epsilon_{\mathbf{q}'} - \epsilon_{\mathbf{k}-\mathbf{q}'}). \tag{49}$$

Using momentum conservation, the energy conservation δ function corresponds to a geometrical condition on the angle θ between $\mathbf{k}$ and $\mathbf{q}'$ (Katz *et al.*, 2002),

$$\cos(\theta) = \frac{1}{2kq'}[k^2 + q'^2 + 1 - \sqrt{(\epsilon_k - \epsilon_{q'})^2 + 1}], \tag{50}$$

where k and q' are in units of ξ^{-1}, and energy is in units of gn. The inset of Fig. 13 shows the energy conserving surfaces in momentum space, for $k\xi$=3.87, 2.49, 1.63, and 1. For momentum values $k\xi \gg 1$ the energy conserving surface is a sphere, as expected from a quadratic dispersion. As $k\xi$ decreases, the surface changes into an oblate lemonlike shape. In the $k \to 0$ limit the surface becomes a straight line, where $\mathbf{q}'$ is parallel to $\mathbf{k}$, as expected from the decay of excitations with a linear dispersion relation.

Converting the sum in Eq. (49) into an integral, and using the above units, the cross section for a Beliaev damping event is given by (Katz *et al.*, 2002)

$$\sigma_k = 8\pi a^2 \frac{1}{2k^2}\int_0^k dq' q' |A_{k,q'}|^2 \frac{\epsilon_k - \epsilon_{q'}}{\sqrt{1 + (\epsilon_k - \epsilon_{q'})^2}}. \tag{51}$$

Figure 13 shows σ_k as a function of k. As seen, the Beliaev damping cross section is largely suppressed at low momenta. There are two reasons for the low k suppression. First, the number of modes q' to which an excitation can damp is significantly reduced as k becomes smaller. Second, A_{kq}, the damping amplitude, is suppressed at low momenta due to quantum interference. The damping cross section, without the contribution of $A_{k,q}$, is indicated by the dashed line in Fig. 13. It is apparent that for most k values, a large fraction of the suppression in the cross section is due to quantum interference rather than a reduction in phase-space density. Contrary to impurity scattering, for which below the superfluid critical velocity, collisions are completely banned (Chikkatur *et al.*, 2000), the cross section for excitation damping, σ_k, is always larger than 0 for $k > 0$. For large k, σ_k approaches $8\pi a^2$, as compared to $4\pi a^2$ for impurities. This enhancement by a factor of 2 is due to boson exchange symmetry.

At a given k we measure the overall probability for an excitation to undergo the first collision p_k. Neglecting secondary collisions, we find that $p_k = N_{\rm count}/N_{\rm mom} - 1$, where $N_{\rm count}$ is the number of observed atoms in the released excitation cloud, and $N_{\rm mom}$ is the measured momentum carried by those atoms (in units of the momentum of a single excitation). This is true since every collision adds another atom to the released excitation cloud, while leaving the total momentum unchanged. p_k is then taken to be equal to $\tilde{n}\sigma_k w_k t_{\rm eff}$, where $t_{\rm eff}$ is the effective interaction time of the excitation with the condensate (during the pulse and during the release), $\tilde{n}$ is the average density, and w_k is the free-particle velocity of the excitations, given by $\hbar k/m$.

The measured ratio, $p_k/(\tilde{n} w_k t_{\rm eff})$ is shown in Fig. 13 and is seen to agree with the theoretical expression for the collision cross section (solid line) calculated as an LDA average of Eq. (51). Due to uncertainties in $t_{\rm eff}$, absolute calibration is not possible, and the experimental points in Fig. 13 have an overall multiplicative factor.

B. Frequency domain—Collisional line broadening and shift

Our considerations in this section have thus far been restricted to the evolution of the excitation population in time. To study the effect of coupling to a quasicontinuum on spectroscopy, one must consider the effect on the excitation energy. As in the time domain, it is useful to employ perturbation theory. We consider an initial state with N excitations in mode k, $|i\rangle = |N_{\mathbf{k}}\rangle$, coupled to a quasicontinuum of final states $|f\rangle$ through $\hat{H}_{\text{int}}$ [Eq. (16)]. $\hat{H}_{\text{int}}$ introduces a shift to an excitation's energy from the Bogoliubov value (Sakurai, 1985),

$$\epsilon(N_{\mathbf{k}}) = N\epsilon_k + N\Delta. \tag{52}$$

$N\Delta$, the energy shift, has both a real and an imaginary part which can be calculated (as a first approximation) in second-order perturbation theory to give

$$\mathrm{Re}(N\Delta) = \mathrm{pr}\sum_f \frac{|\langle f|\hat{H}_{\text{int}}|i\rangle|^2}{(\epsilon_i - \epsilon_f)},$$

$$\mathrm{Im}(N\Delta) = -\pi\sum_f |\langle f|\hat{H}_{\text{int}}|i\rangle|^2 \delta(\epsilon_i - \epsilon_f), \tag{53}$$

where pr stands for the principal part of the sum. The real part of the shift comes from a summation over all possible off-resonance final states, whereas the imaginary part results from a summation over all the on-resonance states. The energy shift of a single excitation can be calculated from Eq. (53) using Eq. (16),

$$\mathrm{Re}(\Delta) = \frac{g^2 N_0}{4V^2}\mathrm{pr}\sum_{\mathbf{q}'}\left(\frac{|2A_{\mathbf{k},\mathbf{q}'}|^2}{2(\epsilon_k - \epsilon_{q'} - \epsilon_{|\mathbf{k}-\mathbf{q}'|})} - \frac{|6B_{\mathbf{k},\mathbf{q}'}|^2}{2(\epsilon_k + \epsilon_{q'} + \epsilon_{|\mathbf{k}+\mathbf{q}'|})}\right), \tag{54}$$

$$\mathrm{Im}(\Delta) = -\pi\frac{g^2 N_0}{4V^2}\sum_{\mathbf{q}'}\frac{1}{2}|2A_{\mathbf{k},\mathbf{q}'}|^2\delta(\epsilon_k - \epsilon_{q'} - \epsilon_{|\mathbf{k}-\mathbf{q}'|}). \tag{55}$$

The numerical prefactors in Eq. (54) and Eq. (55) are due to bosonic exchange symmetry; the amplitudes of indistinguishable final states must be added before squaring.

By comparison with Eq. (49), the imaginary part of Δ can be related to Γ, the Beliaev damping rate, which was calculated from Fermi's golden rule:

$$\mathrm{Im}(\Delta) = -\frac{1}{2}\hbar\Gamma. \tag{56}$$

The evolution of the initial state in time is thus given by

$$|i(t)\rangle = e^{\{-(i/\hbar)[\epsilon_{\mathbf{k}}+\mathrm{Re}(\Delta)]-(\Gamma/2)\}t}|i(t=0)\rangle. \tag{57}$$

The excitation spectrum is given by the Fourier transform of the excitation time-correlation function, defined as

$$c(t=0,t) = \langle i(t=0)|i(t)\rangle = e^{\{-(i/\hbar)[\epsilon_{\mathbf{k}}+\mathrm{Re}(\Delta)]-(\Gamma/2)\}t}. \tag{58}$$

A homogeneous condensate response to the Bragg pulse, as given by Eq. (23), will be modified to (Cohen-Tannoudji *et al.*, 1998)

$$\Gamma_{\mathbf{k}} = \frac{2\pi}{\hbar}\frac{(\hbar\Omega_B)^2}{4}N_0 S_k \frac{\Gamma/2\pi}{\left\{\omega - \frac{1}{\hbar}[\epsilon_k + \mathrm{Re}(\Delta)]\right\}^2 + (\Gamma/2)^2}. \tag{59}$$

Two changes are apparent in the response of a homogeneous condensate to the Bragg pulse due to the coupling to a quasicontinuum. First, the response is shifted by Eq. (54) from the Bogoliubov value. This shift is due to coupling to off-shell momentum modes. An excitation can decay into an off-resonance state. However, since energy is not conserved in such a process, the decay products must recombine to the initial state fast enough that the energy mismatch lies within the energy-time uncertainty. This process will not change the excitation population. However during the round trip to off-resonance final states and back, the excitations acquire a phase shift that is translated into a shift in the resonance energy.

Second, the response of the condensate is broadened from a delta function into a Lorentzian with a full width at half maximum given by Γ, the Beliaev damping rate. This broadening is caused by the finite time an excitation can remain in mode $\mathbf{k}$ before it scatters. This broadening is not caused by inhomogeneity in the condensate, and therefore can be thought of as the "natural" linewidth of the transition. If the Bragg resonance is measured through the observation of the atomic momentum distribution after the pulse (as described in Sec. VI.A), one can measure a linewidth that is narrower than the "natural" linewidth by post-selecting the excitations which did not undergo Beliaev damping (Katz, Ozeri, Rowen, *et al.*, 2004). For most k values, the unscattered excitations are separated from the damping products in the TOF image.

For cigar-shaped inhomogeneous condensates, the broadening of different radial modes due to Beliaev damping requires further investigation (Jackson and Zaremba, 2003).

The line shift is much more difficult to calculate explicitly than is the line broadening, because the sum in Eq. (54) has an ultraviolet divergence, the resolution of which involves subtle questions of renormalization, approximation order, and convergence. The Beliaev correction to the Bogoliubov energy has been calculated for very low-energy states, starting from (Beliaev, 1958), which finds a correction factor of $\sqrt{1+16(na^3/\pi)^{1/2}}$ to the Bogoliubov speed of sound. This factor, for typical experimental conditions, is of the order of a few percent.

More recent treatments applied to gaseous BEC (Fedichev and Shlyapnikov, 1998) involve many different possible approximations beyond second-order perturbation theory. For a complete and critical review of

these results, also see Griffin (1998) and Rogel-Salazar *et al.* (2001).

VIII. WAVE MIXING OF EXCITATIONS

In the previous section the coupling of an occupied mode of Bogoliubov excitations to a quasicontinuum of empty modes was described. Similar to the stimulated emission of photons, the bosonic nature of excitations enables the emphasis of the coupling to a specific mode through its macroscopic occupation. In this final section we will describe the interaction between two macroscopically occupied modes of Bogoliubov excitations.

A. Collisional "power" broadening and "ac-Stark" shift

Our model system is a homogenous condensate of finite volume V, with N_0 atoms in the ground state. We consider the case in which the condensate is excited with N excitations of momentum $\mathbf{k}$ and M excitations of momentum $\mathbf{q}$, $|N_{\mathbf{k}},M_{\mathbf{q}}\rangle$. If $\mathbf{k}$ and $\mathbf{q}$ fulfill the Bragg condition, i.e., $\epsilon_{\mathbf{k}}=\epsilon_{\mathbf{q}}+\epsilon_{\mathbf{k}-\mathbf{q}}$, we refer to the modes as being on-resonance. We define δ, the detuning of mode $\mathbf{q}$, as

$$\delta=\epsilon_{\mathbf{q}}+\epsilon_{\mathbf{k}-\mathbf{q}}-\epsilon_{\mathbf{k}}. \tag{60}$$

In the $\delta=0$ case, the amplitude given by H_{int} for Beliaev damping of the $\mathbf{k}$ momentum excitation into two excitations with momenta $\mathbf{q}$ and $\mathbf{k}-\mathbf{q}$, resulting in a state $|(N-1)_{\mathbf{k}},(M+1)_{\mathbf{q}},1_{\mathbf{k}-\mathbf{q}}\rangle$, will be $\sqrt{M}$-fold larger than any of the other damping channels. This will result in a macroscopic population in the initially unpopulated $\mathbf{k}-\mathbf{q}$ momentum mode. The dynamics between the three macroscopically populated modes is referred to as three-wave-mixing (3WM) of excitations. Experiments along these lines have been performed in the single-particle regime, in which Bogoliubov excitations correspond to single atoms, moving with momentum $\mathbf{k}$. The emergence of a fourth (counting also the 0 momentum mode and therefore usually referred to as atomic four-wave-mixing experiments) macroscopically occupied mode was observed (Deng *et al.*, 1999; Vogels *et al.*, 2003).

Limiting ourselves to a perturbative treatment of the mixing process, the enhanced damping rate per excitation from mode $\mathbf{k}$ can be calculated using Eq. (49),

$$\Gamma=\frac{2\pi}{\hbar}\frac{g^2N_0M}{2V^2}+\frac{2\pi}{\hbar}\frac{g^2N_0}{2V^2}\sum_{\mathbf{q}'}|A_{\mathbf{k},\mathbf{q}'}|^2\delta(\epsilon_{\mathbf{k}}-\epsilon_{\mathbf{q}'}-\epsilon_{\mathbf{k}-\mathbf{q}'}). \tag{61}$$

The Bragg linewidth into mode $\mathbf{k}$ will correspondingly increase. This further broadening of the line is analogous to power broadening of an atomic absorption line, due to the presence of an on-resonance laser beam.

When $\mathbf{k}$ and $\mathbf{q}$ are off-resonance, no real damping will occur from mode $\mathbf{k}$ to mode $\mathbf{q}$. However, the energy of mode $\mathbf{k}$ will be modified. Given that $\delta\ll\epsilon_k$, the contribution of mode $\mathbf{q}$ to the line shift can be approximated by

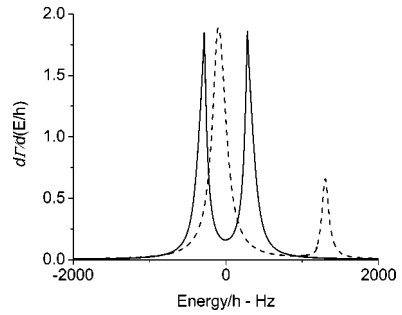

FIG. 14. Beliaev damping spectrum from the $N=M=5\times10^3$, $k=3\ \hbar/\xi$, and $q=k/\sqrt{2}$, dressed-state manifold. The condensate is homogeneous, with 3×10^5 ^{87}Rb atoms and a density of 3×10^{14} atoms/cm^3. The two curves are (solid) for $\delta=0$, and (dashed) $\delta=1.2$ kHz. From Ozeri *et al.*, 2003.

$$\Delta\simeq-\frac{g^2N_0M}{V^2}\frac{|A_{\mathbf{k},\mathbf{q}}|^2}{2\delta}. \tag{62}$$

This shift is analogous to the ac-Stark shift of an atomic line due to the presence of an off-resonance laser beam. This collisional ac-Stark shift can be experimentally observed by measuring the Bragg response for mode $\mathbf{k}$. The sign of the shift depends on the sign of δ.

B. Dressed-state approach

The above perturbative treatment relies on the assumption that the dynamics due to the interaction between excitations in modes $\mathbf{k}$ and $\mathbf{q}$ is overwhelmed by decoherence. For an infinite homogeneous condensate, the only decoherence mechanism present is that of Beliaev damping into the quasicontinuum. In the laboratory, inhomogeneous dephasing mechanisms will be the dominant cause for decoherence. In the case where the dynamics due to the coupling between the modes is faster than the decoherence time of the system, the use of perturbation theory is inadequate, and one would have to solve H_{int} exactly in order to calculate the 3WM dynamics between the various macroscopically populated excitation modes.

One method of finding such an exact solution is the use of a dressed state basis, in which H_{int} is diagonalized (Ozeri *et al.*, 2003). In this basis the 3WM dynamics of the condensate is readily calculated. Excitations are seen to oscillate between the $\mathbf{k}$ momentum mode and the $\mathbf{q}$ and $\mathbf{k}-\mathbf{q}$ momenta modes. In analogy to the treatment of spontaneous photon scattering as transfer between dressed state manifolds of the dressed atom-laser system, Beliaev scattering into empty modes can be treated as transfers between dressed state manifolds. As a result of the 3WM dynamics, Beliaev damping becomes inelastic. The damping spectrum, shown in Fig. 14, is seen to show a splitting that is analogous to the Mollow splitting in the spectrum of photon scattering from a strongly driven atom.

IX. CONCLUSIONS

Bogoliubov and Beliaev theories of excitations in weakly interacting Bose-degenerate gases were developed several decades ago (Bogoliubov, 1947; Beliaev, 1958). The experimental study of BEC, however, is relatively new (Anderson *et al.*, 1995). In the experiments described above, as well as in several other experiments with Bogoliubov excitations in BEC[1] these long awaited "textbook" quantum many-body theories have been verified. Bogoliubov mean-field theory has been proven to provide an extremely accurate framework, within which the time dynamics of weakly interacting condensates can be calculated.

In contrast to many experimental studies of Bogoliubov excitations in BEC, the experiments described here study excitations whose wavelengths are short compared to the condensate size. This regime has two distinctive properties. First, the dynamics of such short-wavelength excitations is dominated by the bulk, intrinsic properties of the condensate, rather than by the condensate geometry. Consequently, the physics of short-wavelength excitations reflects the essence of Bogoliubov quasiparticle theory, as this theory was originally formulated for an infinite homogeneous Bose gas.

Second, Beliaev processes in the short wavelength regime couple excitations to a quasicontinuum of final states. This draws an analogy between the physics of a macroscopically occupied Bogoliubov mode, and that of a macroscopically occupied light mode (a laser), which is coupled to the electromagnetic vacuum through the presence of an atom (Cohen-Tannoudji *et al.*, 1998).

Two photon Bragg transitions are a powerful tool for the experimental study of BEC. There are several future prospects for experiments on condensates, using Bragg transitions. One possibility is the use of Bragg spectroscopy for probing effects that are beyond the Bogoliubov approximation. In this review we have discussed at length the implications of Beliaev dynamics on Bragg spectroscopy. The introduction of strong or long-range interactions into the condensate will require large corrections to the Bogoliubov approximation. Recently there have been several proposals to introduce such long-range interactions by the use of a Feshbach resonance, by irradiating the condensate with strong off-resonance light fields, or by applying strong electric fields to the condensate. Another possibility is to use a condensate of atoms with strong dipolar interactions (Griesmaier *et al.*, 2005). In all of these cases, theoretical predictions have been made for the appearance of second-order density correlations in the condensate, which would form a roton minimum in the condensate excitation spectrum (O'Dell *et al.*, 2003; Santos *et al.*, 2003; Steinhauer *et al.*, 2004). The study of strong Bragg-formed excitations will also require corrections to the Bogoliubov theory. In such a case, the condensate response to the Bragg pulse would be highly nonlinear (Band and Sokuler, 2002; Katz, Ozeri, Rowen, *et al.*, 2004).

Bragg spectroscopy can also be applied to the probing of other condensate states as opposed to the ground state, such as a vortex state (Zambelli *et al.*, 2000; Blakie and Ballagh, 2001), or for the probing of the condensate ground state in nontrivial trapping geometries, such as a double well or an optical lattice (Blakie and Ballagh, 2001; Menotti *et al.*, 2003). In the latter case, Bragg spectroscopy of the Mott insulator phase in an optical lattice could produce insight into number squeezing in this phase (Greiner *et al.*, 2002).

[1]See, for example, Jin *et al.* (1996, 1997), Mewes *et al.* (1996), Stamper-Kurn *et al.* (1998, 1999), Stenger *et al.* (1999), Fort *et al.* (2000), Hodby *et al.* (2001).

ACKNOWLEDGMENTS

We are indebted to Franco Dalfovo and Cesare Tozzo for useful discussions. We thank Wolfgang Ketterle for a critical reading of the manuscript. This work was partially supported by the Israel Science Foundation, the Minerva Foundation, and the DIP program. One of us (N.K.) acknowledges support from the Israeli Ministry of Science.

REFERENCES

Anderson, M. H., J. R. Ensher, M. R. Matthews, C. E. Weiman, and E. A. Cornell, 1995, Science **269**, 198.
Band, Y. B., and M. Sokuler, 2002, Phys. Rev. A **66**, 043614.
Beliaev, S. T., 1958, Sov. Phys. JETP **34**, 323.
Blakie, P. B., and R. J. Ballagh, 2001, Phys. Rev. Lett. **86**, 3930.
Blakie, P. B., R. J. Ballagh, and C. W. Gardiner, 2002, Phys. Rev. A **65**, 033602.
Bogoliubov, N. N., 1947, J. Phys. (Moscow) **11**, 23.
Brunello, A., F. Dalfovo, L. Pitaevskii, and S. Stringari, 2000, Phys. Rev. Lett. **85**, 4422.
Brunello, A., F. Dalfovo, L. Pitaevskii, S. Stringari, and F. Zambelli, 2001, Phys. Rev. A **64**, 063614.
Castin, Y., 2001, in *Coherent Atomic Matter Waves: Lecture Notes of Les Houches Summer School*, edited by C. W. R. Kaiser and F. David (EDP Sciences and Springer-Verlag, Berlin), pp. 1–136.
Chikkatur, A. P., A. Görlitz, D. M. Stamper-Kurn, S. Inouye, S. Gupta, and W. Ketterle, 2000, Phys. Rev. Lett. **85**, 483.
Cohen-Tannoudji, C., J. Doupont-Roc, and G. Grynberg, 1998, *Atom-Photon Interactions* (Wiley, New York).
Cohen-Tannoudji, C., and C. Robilliard, 2001, C. R. Acad. Sci., Ser IV: Phys., Astrophys. **T2**, 445.
Courtois, J.-Y., G. Grynberg, B. Lounis, and P. Verkerk, 1994, Phys. Rev. Lett. **72**, 3017.
Dalfovo, F., S. Giorgini, L. P. Pitaevskii, and S. Stringari, 1999, Rev. Mod. Phys. **71**, 463.
Davis, K. B., M.-O. Mewes, M. R. Andrews, N. J. van Druten, D. S. Durfee, D. M. Kurn, and W. Ketterle, 1995, Phys. Rev. Lett. **75**, 3969.
Deng, L., E. W. Hagley, J. Wen, M. Trippenbach, Y. Band, P. S. Julienne, J. E. Simsarian, K. Helmerson, S. L. Rolston, and W. D. Phillips, 1999, Nature (London) **398**, 218.
Edwards, M., P. A. Ruprecht, K. Burnett, R. J. Dodd, and C. W. Clark, 1996, Phys. Rev. Lett. **77**, 1671.

Einstein, A., 1925, Sitzungsber. Preuss. Akad. Wiss., Phys. Math. Kl. **1**, 3.
Fedichev, P. O., and G. V. Shlyapnikov, 1998, Phys. Rev. A **58**, 3146.
Fetter, A. L., 1998, in *Proceedings of the International School of Physics "Enrico Fermi," Course CXL*, edited by M. Inguscio, S. Stringari, and C. E. Wieman (IOS, Amsterdam), p. 201.
Fort, C., M. Prevedelli, F. Minardi, F. S. Cataliotti, L. Ricci, G. M. Tino, and M. Inguscio, 2000, Europhys. Lett. **49**, 8.
Gershnabel, E., N. Katz, R. Ozeri, E. Rowen, J. Steinhauer, and N. Davidson, 2004, Phys. Rev. A **69**, 041604.
Gershnabel, E., N. Katz, E. Rowen, and N. Davidson, 2004, New J. Phys. **6**, 127.
Giorgini, S., 1998, Phys. Rev. A **57**, 2949.
Greiner, M., O. Mandel, T. Esslinger, T. W. Hänsch, and I. Bloch, 2002, Nature (London) **415**, 39.
Griesmaier, A., J. Werner, S. Hensler, J. Stuhier, and T. Pfau, 2005, cond-mat/0503044.
Griffin, A., 1993, *Excitations in a Bose-Condensed Liquid* (Cambridge University Press, Cambridge, Great Britian).
Griffin A., 1998, in *Proceedings of the International School of Physics "Enrico Fermi," Course CXL*, edited by M. Inguscio, S. Stringari, and C. E. Wieman (IOS, Amsterdam), p. 591.
Gross, E.P., 1961, Nuovo Cimento **20**, 454.
Hagley, E. W., L. Deng, M. Kozuma, M. Trippenbach, Y. B. Band, M. Edwards, M. Doery, P. S. Julienne, K. Helmerson, S. L. Rolston, and W. D. Phillips, 1999, Phys. Rev. Lett. **83**, 3112.
Hodby, E., O. M. Maragò, G. Hechenblaikner, and C. J. Foot, 2001, Phys. Rev. Lett. **86**, 2196.
Hutchinson, D. A. W., and E. Zaremba, 1998, Phys. Rev. A **57**, 1280.
Jackson, B., and E. Zaremba, 2003, New J. Phys. **5**, 88.
Jin, D. S., J. R. Ensher, M. R. Matthews, C. E. Wieman, and E. A. Cornell, 1996, Phys. Rev. Lett. **77**, 420.
Jin, D. S., M. R. Matthews, J. R. Ensher, C. E. Wieman, and E. A. Cornell, 1997, Phys. Rev. Lett. **78**, 764.
Katz, N., R. Ozeri, E. Rowen, E. Gershnabel, and N. Davidson, 2004, Phys. Rev. A **70**, 033615.
Katz, N., R. Ozeri, J. Steinhauer, N. Davidson, C. Tozzo, and F. Dalfovo, 2004, Phys. Rev. Lett. **93**, 220403.
Katz, N., J. Steinhauer, R. Ozeri, and N. Davidson, 2002, Phys. Rev. Lett. **89**, 220401.
Ketterle, W., and S. Inouye, 2001, C. R. Acad. Sci., Ser IV: Phys., Astrophys. **2**, 339.
Kozuma, M., L. Deng, E. W. Hagley, J. Wen, R. Lutwak, K. Helmerson, S. L. Rolston, and W. D. Phillips, 1999, Phys. Rev. Lett. **82**, 871.
Landau, L. D., 1941, J. Phys. (Moscow) **5**, 71.
London, F., 1938, Nature (London) **141**, 643.
Matthews, M. R., D. S. Hall, D. S. Jin, J. R. Ensher, C. E. Weiman, E. A. Cornell, F. Dalfovo, C. Minniti, and S. Stringari, 1998, Phys. Rev. Lett. **81**, 243.
Menotti, C., M. Krämer, L. Pitaevskii, and S. Stringari, 2003, Phys. Rev. A **67**, 053609.
Mewes, M.-O., M. R. Andrews, N. J. van Druten, D. M. Kurn, D. S. Durfee, C. G. Townsend, and W. Ketterle, 1996, Phys. Rev. Lett. **77**, 988.
Morgan, S. A., S. Choi, K. Burnett, and M. Edwards, 1998, Phys. Rev. A **57**, 3818.
Nozières, P., and D. Pines, 1990, *The Theory of Quantum Liquids* (Addison-Wesley, Reading, MA), Vol. II.
O'Dell, D. H. J., S. Giovanazzi, and G. Kurizki, 2003, Phys. Rev. Lett. **90**, 110402.
Onofrio, R., D. S. Durfee, C. Raman, M. Köhl, C. E. Kuklewicz, and W. Ketterle, 2000, Phys. Rev. Lett. **84**, 810.
Ozeri, R., N. Katz, J. Steinhauer, E. Rowen, and N. Davidson, 2003, Phys. Rev. Lett. **90**, 170401.
Ozeri, R., J. Steinhauer, N. Katz, and N. Davidson, 2002, Phys. Rev. Lett. **88**, 220401.
Perez-García, V. M., H. Michinel, J. I. Cirac, M. Lewenstein, and P. Zoller, 1996, Phys. Rev. Lett. **77**, 5320.
Pitaevskii, L., and S. Stringari, 1997, Phys. Lett. A **235**, 398.
Pitaevskii, L. P., 1961, Sov. Phys. JETP **13**, 451.
Plischke, M., and B. Bergersen, 1994, *Equilibrium Statistical Physics*, 2nd ed. (World Scientific, Singapore).
Richard, S., F. Gerbier, J. H. Thywissen, M. Hugbart, P. Bouyer, and A. Aspect, 2003, Phys. Rev. Lett. **91**, 010405.
Rogel-Salazar, J., G. H. C. New, S. Choi, and K. Burnett, 2001, J. Phys. B **34**, 4617.
Rogel-Salazar J., S. Choi, G. H. C. New, and K. Burnett, 2004 J. Opt. B **6**, R33.
Sakurai, J. J., 1985, *Modern Quantum Mechanics* (Addison-Wesley, Reading, MA).
Santos, L., G. V. Shlyapnikov, and M. Lewenstein, 2003, Phys. Rev. Lett. **90**, 250403.
Simsarian, J. E., J. Denschlag, M. Edwards, C. W. Clarck, L. Deng, E. W. Hagley, K. Helmerson, S. L. Rolston, and W. D. Phillips, 1999, Phys. Rev. Lett. **85**, 2040.
Stamper-Kurn, D. M., A. P. Chikkatur, A. Görlitz, S. Inouye, S. Gupta, D. E. Pritchard, and W. Ketterle, 1999, Phys. Rev. Lett. **83**, 2876.
Stamper-Kurn, D. M., H.-J. Miesner, S. Inouye, M. R. Andrews, and W. Ketterle, 1998, Phys. Rev. Lett. **81**, 500.
Steinhauer, J., N. Katz, R. Ozeri, N. Davidson, C. Tozzo, and F. Dalfovo, 2003, Phys. Rev. Lett. **90**, 060404.
Steinhauer, J., R. Ozeri, and N. Davidson, 2004, cond-mat/0303375.
Steinhauer, J., R. Ozeri, N. Katz, and N. Davidson, 2002, Phys. Rev. Lett. **88**, 120407.
Stenger, J., S. Inouye, A. P. Chikkatur, D. M. Stamper-Kurn, D. E. Pritchard, and W. Ketterle, 1999, Phys. Rev. Lett. **82**, 4569.
Stringari, S., 1996, Phys. Rev. Lett. **77**, 2360.
Stringari, S., 1998, Phys. Rev. A **58**, 2385.
Tisza, L., 1938, Nature (London) **141**, 913.
Torii, Y., Y. Suzuki, M. Kozuma, T. Sugiura, T. Kuga, L. Deng, and E. W. Hagley, 2000, Phys. Rev. A **61**, 041602.
Tozzo, C., and F. Dalfovo, 2003, New J. Phys. **5**, 54.
Tozzo, C., and F. Dalfovo, 2004, Phys. Rev. A **69**, 053606.
Vogels, J. M., J. K. Chin, and W. Ketterle, 2003, Phys. Rev. Lett. **90**, 030403.
Vogels, J. M., K. Xu, C. Raman, J. R. Abo-Shaeer, and W. Ketterle, 2002, Phys. Rev. Lett. **88**, 060402.
Zambelli, F., L. Pitaevskii, D. M. Stamper-Kurn, and S. Stringari, 2000, Phys. Rev. A **61**, 063608.